7   Auxiliary Devices, Calculations, and Construction

7.1   Control Drives

The most important process drives are speed-, tension- or throughput-controlled, and are differentiated (Table 7.1) into:

- continuously-adjustable, either manually or electrically,
- sensor-driven control drives,
- self-regulating drives.

7.1.1   Mechanically Adjustable and Control Drives (Table 7.1)

These are further differentiated according to the type of speed setting/control:

- Change gear and change (toothed)-pulley drives. These are used when the production speed will remain constant for a given product for a long time, but needs to be changed from time to time when the product changes, as, for example, with drawtwisters and draw texturizing machines. These drives only permit changes in small discrete steps, but are exact and remain constant. Finer gear gradations require a two-stage gearbox, comprising, e.g., 50% or 100% change gears.
- Mechanical control drives, in common with change gear drives above, deliver higher torque at lower speeds. Their uniformity and reproducibility are, however, no better than $\pm 0.3\%$ for PIV (positively infinitely variable) drives and $> \pm 0.5\%$ for friction roll drives. Additionally, their maximum output speed is limited to a few thousand revs/min [15].
- This group includes:
  - PIV gearboxes (Fig 7.1 [10]), which use a toothed- or toothed roller-chain that grips in two adjustable toothed conical disks. These drives have an output power of from ca. 0.25 kW to a few hundred kW and are adjustable over a range of 1:6.
  - Steel conical friction roll gearboxes, from, e.g., Heynau [7] and PIV for low power drives. Friction conical wheel control gearboxes, among others, for low power drives [7, 10, 11], adjustable over a range of up to 1 : 10.
  - Mechanical shift gearboxes, e.g., Gusa gearboxes or "Harmonic Drives". Because of the gear play required for changing gears, these drives do not always run truly round [6].
  - Adjustable belt drives, in which a (special) V-belt runs between a normal pulley and an adjustable-gap, two disk conical pulley, the speed adjustment being made by spring pressure, which opens or closes the gap, thereby altering the pulley diameter [10, 9, 3].

7.1.2   Control Motors (Table 7.1)

There are many different types of electric motors:

- Parallel-wound (shunt) DC motor, mostly with additional series-windings to increase starting torque. These are frequently used for spinning extruders up to 400 kW or for fiber draw lines up to 1000 kW,

Table 7.1 Control Drives, Motor Types, Power Supply and Working Ranges

Type	Speed/control range determinant	Power range in kW	Power source	Rotational speed range	Speed accuracy	Control range	Direction of rotation	Examples of application
Belt drives [3, 10]	$\phi 1 : \phi 2$	$0.25 \ldots \approx 40$	AC motor	$300 \ldots 3000$	0.5%	$6 \ldots 10$	r./l.	Robust, subordinate drives
Chain drives [10]	$\phi 1 : \phi 2$	$0.6 \ldots \approx 150$	AC motor	$300 \ldots 2200$	1.5%	$4 \ldots 6$	r./l.	Robust, relatively accurate drives
Geared rolls [7]	$\phi L1 : \phi L2$	$0.6 \ldots \approx 6(75)$	AC motor	$(0)300 \ldots 3000$	2%	$9 \ldots$	r./l.	Small drives
Gearbox drives [6]		$0.12 \ldots \approx 10$	AC motor	$0 \ldots 225$		~ 6	l.	Not rotationally exact
Parallel-wound (shunt)	Armature voltage	$1 \ldots 1300$	1 Q thyristor	$20 \ldots 3000$	1.5%	<100	r.; l. on reversal of field current	Spin extruder
DC motor [12, 1, 4]			4 Q thyristor	$30 \ldots 2800$	1.0%	<100	r./l. with reversal of armature voltage.	Draw frame drives
AC slip ring motor	Rotor voltage	$20 \ldots 2000$	Mains	$600 \ldots 3000$	1.5%	$1.3 \ldots 4.5$	l.	
AC squirrel-cage induction motor	Standard frequency and voltage	$0.04 \ldots 2800$	Frequency inverter	$2 \ldots 1200$ $(\ldots 24000)$	1.0%	$10 \ldots 100$	r./l.	Replacement for DC drives
	As above, with digital speed control	$1 \ldots 20$	Frequency inverter	$500 \ldots 7000$	0.1%	8	r./l.	Draw rolls for coarse titer
AC reluctance motor [8, 12]	Frequency	$0.2 \ldots 6/50$ Hz	Frequency inverter	$200 \ldots 1200$	0.01% or	8	r./l.	Draw rolls, spin pumps
AC permanent magnet motor [12]	Frequency	$0.28 \ldots 2.35/50$ Hz	Frequency inverter	$200 \ldots 1500$ $(\ldots 24000)$	$<0.1\%$[1]	8	r./l.	Draw rolls etc. and frictional drives

AC = alternating current; DC = direct current; Q = quadrant
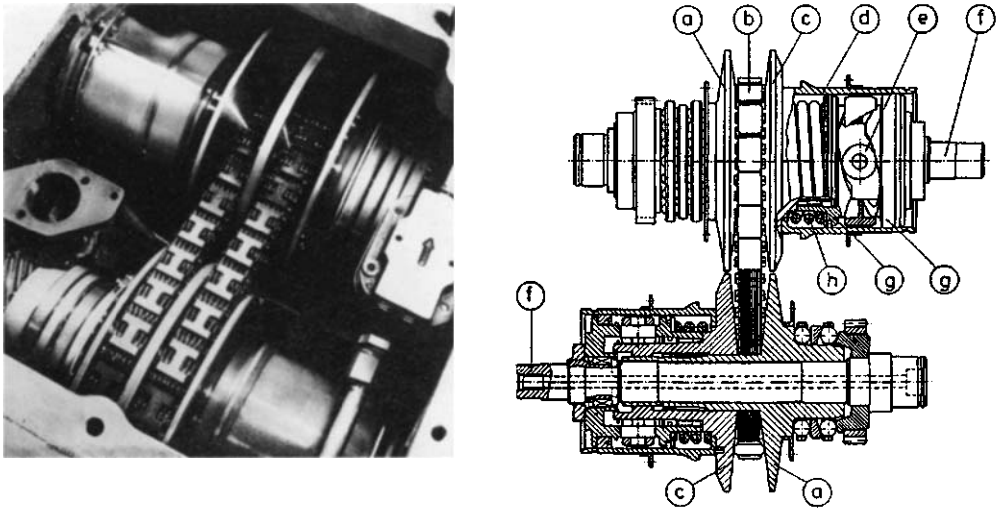[1] Depending on frequency inverter, up to better than 0.01%

Figure 7.1   PIV Variable Drive Gearbox RH 10; left: top view into housing; right: schematic [10].

a) Fixed disk   e) Contact roll
b) Chain   f) Shaft
c) Engaging/disengaging disk   g) Cam
d) Pressure cylinder   h) Pressure spring

although there is a tendency to replace them with regulated AC motors. Disadvantages are their maintenance costs and the need to replace worn parts (commutator and carbon brushes). The usual enclosure class P22 can cause problems when used under moist or wet conditions. Because of cooling requirements, higher protection classes necessitate larger constructions, although protection up to "extra dry" is possible [16]. Control accuracy and reproducibility of from 0.5% to 0.1% is possible, but the extra costs are only justifiable for larger motors.

- The AC squirrel-cage induction motor, available in all sizes and protection classes, is the most widely used drive motor. It exhibits load-dependent slip, both when mains-operated and/or when driven by a frequency inverter. Speed constancy and reproducibility are only $1 \ldots 1.5\%$; this can be significantly improved by means of auxiliary controllers. For speeds above 3000 rev/min for 50 Hz, there is no alternative. By fitting an additional digital tachometer, the precision can be improved to 0.1% [3,17], so that it can be used for yarns of high titer and for duo (godet roll pair) drives, but is, however, still not exact enough for textile yarns.

- Reluctance motors are AC motors having a stator with an AC winding and distinct poles. They always have an even number of pole pairs, stable settings and, after acceleration, run in synchronization with the mains supply. On being externally loaded, reluctance motors run with a lag (slip), the lag angle depending on the load. This is, in practice, of no consequence. Fitted with a short-circuiting ring in the rotor cage, these motors accelerate asynchronously then jump into synchonization at their slip speed. The pull-in torque is normally designed to be 150% of the nominal torque [18]. The power factor is normally $\cos \varphi \approx 0.4 \ldots 0.5$; in particularly well designed versions, $0.63 \ldots 0.68$ can be achieved [18]. The efficiency of $\eta = 0.8 \ldots 0.9$ corresponds to that of an asynchronous motor of equivalent power. For >180 Hz shaft frequency, special dynamo blades must be used, otherwise self-induction would prevent attainment of high power (at high rotational speed). The reluctance motor is particularly suited for use with static frequency inverters, where its speed accuracy depends only on the frequency accuracy of the inverter: a 16-bit control enables an accuracy of $\leq 0.01\%$ to be achieved. Here it is essential to have the V/f (Volts/Hz) characteristic of the inverter in the form of a 4-point polygon, fitted between 0 and the nominal frequency. Figure 7.2 compares the characteristic curves of a reluctance motor and a squirrel cage motor. The start-up current of a reluctance motor is 7 to 8 times that of a squirrel cage motor. When only one reluctance motor is
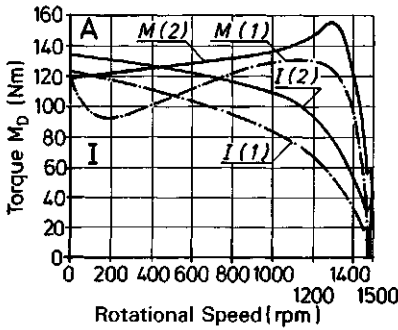
Figure 7.2   Comparison of the characteristic curves of a normal squirrel cage induction motor (1) and a reluctance motor (2), here size 132 M4 according to DIN 42673

Figure 7.3
Operating curves of a permanent magnet synchronous motor (for a winder friction drive roll, average values derived from data in [12]).

Rotational speed n (r/min) $= 30 \cdot f\,[\mathrm{s}^{-1}]$
Pull-out torque $= 1.6 \times$ nominal torque
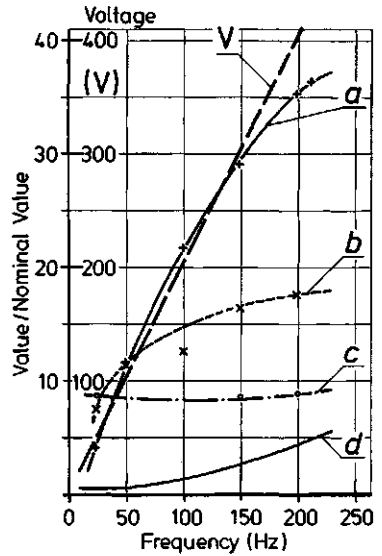Pull-in torque $= 0.36 \times$ nominal torque
Starting torque $= (2.5 \ldots 4) \times$ nominal torque
a) Starting current
b) Operating current
c) Nominal (rated) current
d) Idling current

connected to the inverter, it can be accelerated at the limiting current of the inverter. The use of reluctance motors is recommended, particularly when a small number of synchronous motors is involved.

- The permanent magnet motor [1,2,12] is constructed in the same way as a normal AC asynchronous motor, but has, in addition to the cage start-up winding in the rotor, specially-constructed magnetic paths and gaps filled with non-magnetic material (Fig. 7.4). The permanent magnet excitation (according to the manufacturer) results in better operating characteristics (cos φ and η) and up to 50% reduced current during steady operation, but also in an approx. 16-fold increase in start-up current
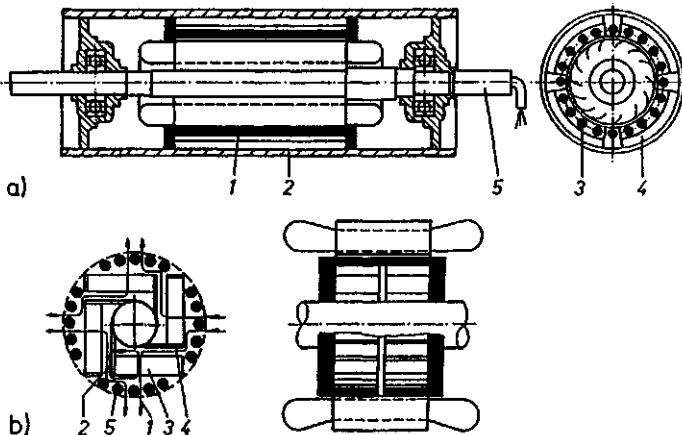

Figure 7.4   Schematic design of:
a) a 4-pole Siemosyn motor [12]:
    1 Permanent magnet flux
    2 Stray flux
    3 Ferrite block magnets
    4 Non-magnetic gaps
    5 Squirrel cage rods and short-circuit ring
b) a Siemosyn external rotor motor of a winder friction drive roll
    1 Stator
    2 Drum casing, including rotor
    3 Squirrel cage rods and short-circuit ring
    4 Permanent magnets
    5 Stationary shaft

(Fig. 7.3). These motors are particularly recommended when a large number of motor drives are required for *spinning pump* drives (4.6.11), draw roll drives (section 4.9.3.1) and friction winder drive rolls (section 4.9.5.1, Figure 7.4). The V/f (V/Hz) ratio must be set so that ca. 95% of the inverter mains supply voltage is not exceeded. Also, the max. permissible externally-applied torque given in Fig. 7.5 must not be exceeded in order to allow the self-accelerating synchronous motor to jump into synchronization. Two pole synchronous motors should only be used when the required speed of $\geq 5500 \ldots 6000$ r/min necessitates their use, otherwise 4-pole motors should be used.
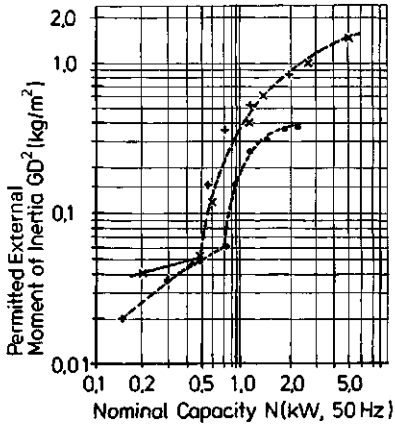

Figure 7.5 Allowable externally-applied moment of inertia (e.g. of draw rolls) GD^2 for "Siemosyn" motors (Compiled from tables given in [12])

- Small synchronous (geared) motors [20] of $20 \ldots 80$ W are used for driving small aggregates, e.g., spin finish pumps, where, e.g., 4- or 6-pole flange motors with gear-down ratios of $1:10$ to $1:1000$ and of 40 or 60 W are used for a speed range of $12 \ldots 80$ r/min.
- DC-excited synchronous motors have lower starting currents than the motors described above, but are nowadays hardly used [21].

7.1.3   Current Converters and Inverters

The above-described motors only become control drives when connected to appropriate, adjustable current converters. Their speed accuracy depends on the combination. Only in the case of synchronous motors is the frequency inverter accuracy alone decisive. Table 7.2 gives an overview of the most important devices (taken from [12]).

Today DC shunt-wound motors are still preferred for control drives of ≥ 100 kW, sometimes fitted with additional series-windings to assist start-up. According to the VDE (German electrotechnical association), an overload factor of 1.5 should be sustainable for 60 s. The standard armature voltages are 150, resp. 260 V for single phase thyristor sets using 220, resp. 380 V mains supply and 400 resp. 440 V for 3-phase sets using 380 V supply with 4-, resp. 1-quadrant operation. A smoothing choke is not required only when the nominal motor speed < maximum motor speed [74, 75].

The approximately wave-shaped output voltage must be taken into consideration in the dimensioning of the system. The best option is a thyristor having a 6-pulse upper voltage wave: this requires a current factor of 1.25 to 1.10. Less favourable are semi-regulated three-phase current bridge switches or semi- and fully-regulated single phase bridges with current factors of $1.30 \ldots 1.72$, which can be reduced to $1.15 \ldots 1.25$ by means of a smoothing choke. The latter should only be used for motors of ≤ 5 kW. The control range is also influenced by the stop/start frequency and the quality of the motor cooling.

Table 7.2   Control Motors and Thyristor Sets [12]

Converter	Single phase transformer	two phase transformer	indirect inverter
Motor	Parallel-wired (shunt) DC motor		Synchronous AC motor and special case motor
Speed determining factors	Motor armature voltage. If necessary, also motor field voltage		Stator frequency and voltage
Principle of speed adjustment	Control of armature voltage via regulated line transformer		Control or regulation of the stator frequency via machine- based, self regulating transformer; controlled adjustment of the stator frequency via regulated mains transformer
Control execution	Fully-digital microprocessor controller with standardized interfaces (optional analog control with hybrid integrated circuit)		
Typical speed adjustment range or frequency range in the case of AC	1 : 100	1 : 100	1 : 10
Principle of torque reversal	Reversal of the field current via external contactors	Reversal of the armature current electronically	Reversal of the indirect current
Typical application	One direction, motoring	Two direction motoring and braking	Two directions, motoring
Typical applications after modification	Resistance braking	Braking by means of controlled resistance or impedance under pulse resistance or via anti-parallel line-powered current (depending on the series)	
Typical power range	1 ... 1300 kW (G)	2 ... 1250 kW (G)	0.40 ... 380 kVA (G)
G = equipment series	... 10 000 kW and larger	... 10 000 kW and larger	
Typical characteristics	Reduced transformer expenditure; limited torque reversal frequency	High performance control dynamics	High inverter frequencies, high frequency constancy and reproducibility, stable in no-load operation, can tolerate 50% over load for 60 s
Main fields of application	All types of process machinery	Cranes, drawstands, paper-, plastic- and textile machines, machine tools	Preferred for group drives e.g., textile machines, fans

The required thyristor sizing for DC motors can be calculated from:

$$I_{\text{Typ,catalog}} \geq I_{\text{motor}} \cdot f \cdot (1 + a_x \cdot R_x) \cdot f_t \cdot k_z,$$

where: $f =$ upper voltage wave factor
$R =$ control range
$x = 1: a_x = 0.1$ for solid yoke motors
$x = 2: a_x = 0.33$ for sheet metal-encased motors

$f_t =$ factor for environment temperature	=	1	1.05	1.1	1.16	1.24
for a motor environmental temperature of		40	45	50	55	60 °C
$k_z =$ correction factor for start/stop operation	=	0.6	0.7	0.8	0.9	
for a starting frequency of		16	25	40	60%.	

Even in the most favorable cases, there is a current factor of 1.25 between the motor and the thyristor set [75]. For DC motor drives, one transformer per motor is usually used. Braking action, whether caused by stretching tensions in fiber draw lines or by stopping the machine, must be calculated as above. Here, however, the current generated must either be dissipated through resistances or must be fed to other thyristors.

In the case of frequency-controlled drives, it is possible to use one inverter per motor and, when required, to couple many motors to the same frequency for constant speed operation, or to supply many motors running at the same speed from a common inverter, for example for spinning pump drives or draw roll motors in a drawtwister, etc.

The following comparison is therefore made (for 12 motors):

Single inverter per 1 motor   Common inverter for n motors

$I \geq 4\, I_{\text{motor, nom}}$ $I \geq (n - 1)\, I_{\text{motor running, max}} + I_{\text{motor start, max}}$

Example: 12 friction rolls at 6000 m/min: $I_{\text{nom}} = 4.5$ A; cos $\varphi = 0.8$; $I_{\text{running, max}} = 4.16$ A;
$I_{\text{starting, max}} = 77.5$ A at $f = 212$ Hz

per motor: $I \geq 4 \cdot 4.16/0.8 = 20.8$ A

Total: $I_{\text{total}} \geq 12 \cdot 20.8 \approx 250$ A   Total: $I = (11 \cdot 4.16 + 77.5)/0.8 \approx 154$ A

$N_{\text{total}} \approx 216$ kW (at 424 V) $N \approx 43$ kW, or
1 · as left, to start: 20.8 kW
$+ 12 \cdot 13.75$ kW $= I_{\text{total}} = 185.8$ A

Operating results:
$I_{\text{op}} = 12 \cdot 4.66/0.8 \approx 63$ A $I_{\text{op}} \approx 64$ A

The sample calculation using 12 motors clearly shows the common inverter to be advantageous. This can be taken for granted when using more than 6 motors, but must be checked for the case of 4 motors. The advantages and disadvantages of both systems are, additionally:

- if one inverter trips out, remaining 11 continue to operate
- easy exchange of modular cards
- interference in mains and line caused by sine pulse approximation
- n single controllers

- cost advantageous for up to 4 or 5 synchronous motors running at same speed

- a trip out stops the entire system

- exact sine wave current

- only a single controller, which can therefore be designed to give greater process security. cost advantagous for >6 to 8 synchronous motors per inverter, unless there are other reasons which require the use of single inverters.

Rapid braking can also be important in many processes, as in the stopping of full packages or draw rolls, or in wobbling. The latter involves a fairly strong increase and decrease in the rotational speed of the traverse of up to 5% using frequencies of 0.5 ... 0.05 Hz derived from a given curve. In the case of single

inverters, the braking energy must be dissipated, e.g., by means of a ballast resistance (ca. 30 Ω at 11 kW); a common inverter can absorb this. The control cabinet temperature must not be allowed to rise above 35 (...40) °C. This may possibly require external, forced cooling.

For further dimensioning of the frequency inverter, account must be taken of:

- maximum voltage of the frequency-regulated circuit: $U_{max} = U_{line} -$ ca. 20 V (e.g., for a line of 3×380 V: max. 360 V)
- maximum frequency: using an 8 kHz carrier frequency, an output frequency of 300 Hz can be achieved without too large a loss, as long as the motor dynamo plates permit this, otherwise the self-induction losses above ca. 200 Hz are too large.
- a U/f ratio of max. ca. 2.5 V/Hz should not be exceeded; e.g., 360 V/212 Hz ≈ 1.7 V/Hz.
- The current is given by $I = N/U \cdot \sqrt{3} \cdot \cos\varphi$, and should be $I_{design} \geq 4 \cdot I_{max}$ (· 1.1, recommended) > current at locking-in torque.

For operational safety reasons, static inverters must meet the following requirements [3]:

- set point potential separation, e.g., by means of a light wave conductor and- coupler (LWL technology)
- electronic overload protection during short-circuiting and earthing. Fuses which melt are no longer sufficient.
- over-voltage protection.
- high overload factor, i.e., high quality power circuit
- generously-dimensioned intercircuit condenser.
- no automatic re-starting after error correction
- if possible, operation without forced air cooling.
- contact protection according to DIN-VDE 0160 [88]
- stored chopper-mains component for on-going bridging of short-term mains interruptions
- temperature monitoring of power components
- least possible mains interference during error correction.
- as far as possible, continuous interference suppression according to VDE 0871
- protection class IP54, incorporated into control cabinet construction.

In addition, the static frequency inverter must include the following differentiated fault alarms:

- intercircuit overvoltage, short circuiting and earthing
- motor over-temperature, in conjunction with motor cold conductor monitoring.
- over-temperature in power circuits.
- overload in motoring- and generating modes.
- motor stator frequency.

The standard accuracy of ± 0.5% is sufficient for the following drives: spin extruders, spin finish rolls or pumps, traverse mechanisms and dancer-roll-controlled package winding. In contrast, drives for spinning pumps, draw rolls and winder friction drive rolls, amongst others, require an accuracy of better than ± 0.01%. The latter accuracy is also required for the yarn delivery systems of drawtwisters, draw-winders and drawtexturizing machines.

Figure 7.6 shows the circuit diagram of a dancer-roll-controlled package winder equipped with a hyperbolic controller for regulating the frequency converter, which requires an additional 0...10 V signal [3].

A machine having 2 or more synchronous motors can only be designed according to the principle of single inverters when these motors are electrically equivalent and are accelerated together at maximum current to their common operating speed. Using the motor data given in Table 7.3, there are three possible layout configurations for a godet duo (drawroll pair):

- two frequency inverters for two motors in independent operation: A, $N \geq$ each (3.4 A or 0.6 kW) · 4 = 13.6 A or 2.4 kW per inverter
- one frequency inverter for starting both motors (only) together: A, $N \geq (2 \cdot 3.4$ A or $2 \cdot 0.6$ kW) · 4 = 27.2 A or 4.8 kW.
- one frequency inverter for two motors : either motor can be switched to the status of the other (stopped/running): A, $N \geq (3.4 + 32)$ A or $(0.6 + 13)$ kW = 35.4 A or 13.6 kW.
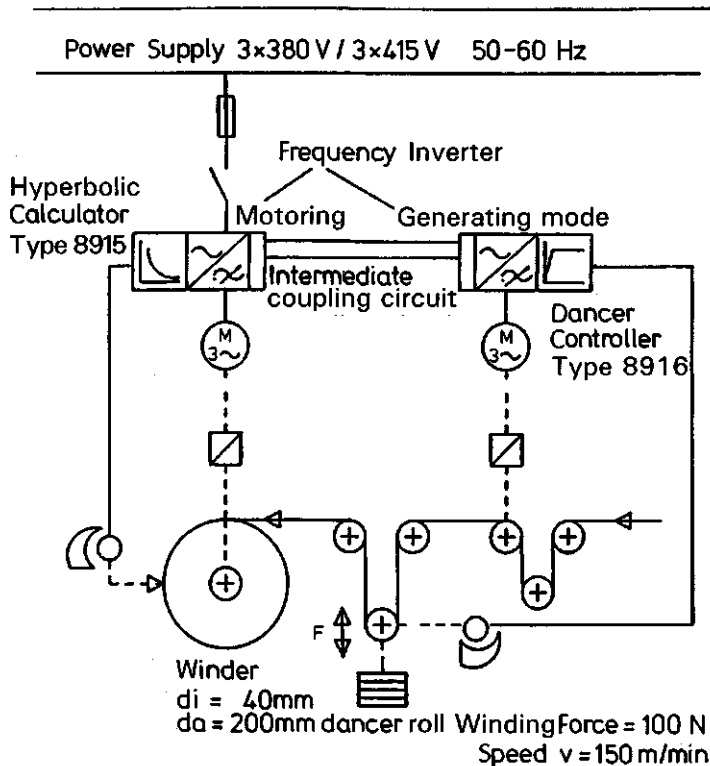
Figure 7.6   Yarn winder with speed/yarn tension control via a dancer roll, using an asynchronous motor [3]

Table 7.3   Examples of Data for the Siemens "Siemosyn" Motor, Type A68/91/145: 2-pole [12]

Frequency	50	100	150	200	230	Hz
Voltage	90	180	270	360	414	V
Nominal current	2.9	3.0	3.1	3.3	3.4	A
Operating current	1.92	2.07	2.15	2.25	2.40	A
Starting current	13	21	27	30	32	A
Operating power	56.3	108.2	223.6	394.6	553.9	W
Starting power	1516	4326	7891	10850	12981	W

The first two solutions are technically equivalent; the third results in too large an inverter, but—like the first solution—allows each godet to be started and stopped independently.

7.2   Yarn Guides, Spin Finish Applicators, and Yarn Sensors

These items are used to converge and guide yarns. The most important materials of construction are sapphire (seldomly used), sintered aluminum oxide (Al_2O_3), hard coated hardened steel and glazed porcelain. The most important materials are given in Table 7.4. The coefficient of friction of yarn running over a yarn guide is strongly dependent on the fiber type (Fig. 7.7a), the guide material and its coating or surface treatment, the spin finish (section 6.7.2) and the fiber delusterant. Natural Al_2O_3 yarn guides are white; a small amount of chrome oxide colors them ruby red.

Table 7.4   Construction Materials for Yarn Guides and Spin Finish Applicators

Material properties		Steel		Sintered material Al_2O_3	Porcelain, glazed
		hard-chromed	Surface plasma coated		
Density	[g/cm^3]	7.85	7.85/3.4	3.9	~2.4
Vickers Hardness (HV, 500 g)			1100	1750	
Bending strength	[MPa]			300...450	
Thermal expansion coefficient between 20...500°C	[10^{-6}/K]			7.5	
Thermal conductivity 20°C	[W/mK]	30	30	30	20...25
Specific heat c_p	[J/g·K]			0.9	
Max. application temperature	[°C]	160	250	1500	
Electrical resistivity at 20°C	[Ω·cm]			10^{14}	
at 120°C				10^{8}	
Comparative frictional coefficient		0.23...0.35	0.2...0.4	0.25...0.4	0.3...0.8
range at roughness Ra	[μm]	~0.1	~0.25	≈0.3	<0.1
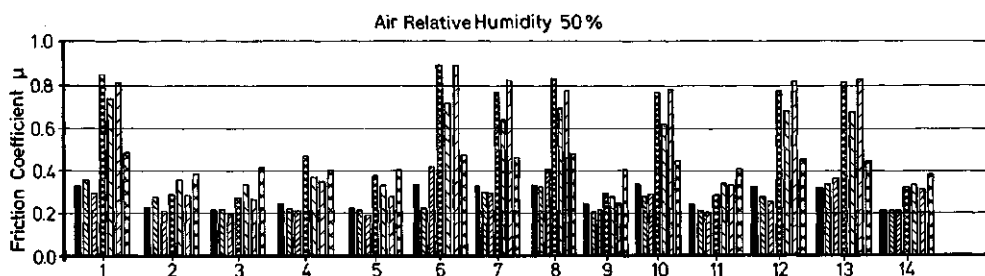
Figure 7.7a   Friction coefficient between various yarn guide materials at 50% R.H. and various fiber types [24].
Yarns:

■	Vetrotex 60 tex Z28	(hatched)	Vetrotex 34 tex Z28
(cross)	Kevlar 29 200 den	(diag)	Kevlar 49 380 den
(X)	Carbon Tenax W 1000	(diag)	Silenka 34 text Z40
		(open)	Twaron 420 dtex f 1250

Yarn guides:

1 Aluminum oxide "Rapal", polished
2 Aluminum oxide "Rapal", ground and scoured (tumbled)
3 Aluminum oxide "Rapal", "as is", scoured (tumbled)
4 Titanium dioxide Ta 11, "as is", scoured (tumbled)
5 TiO$_2$, ground and scoured (tumbled)
6 TiO$_2$, polished
7 Porcelain, white, glazed

8 Porcelain, brown, glazed
9 Porcelain, matt-blue, glazed
10 Porcelain, green, glazed
11 Ceramic coated
12 Ceramic coated and polished
13 Zircon oxide
14 Hard chrome, matt, on steel

The surface roughness of Al_2O_3 in its natural state is $R_a \approx 0.4...0.9$ μm, polished Al_2O_3 has an $R_a \approx 0.15...0.3$ μm and the surface roughness of the often-preferred matt silk finish lies inbetween these values.

The gliding speed of yarn over a guide or yarn brake has an effect on the braking force, as can be seen in Fig. 7.7b for various guide materials and yarns. The lowest friction is also associated with the lowest electrostatic charge. Most results available in the literature are ill-defined, omitting to mention, among others, inlet tension, test conditions, spin finish, etc.. The twist separation method gives the most reliable results, though only similar or identical textile materials can be used.

Figure 7.8 gives a frequently-used selection of yarn guides from the many forms available from manufacturers' catalogs, while Fig. 7.9 shows a similar selection of spin finish applicators [23–26,
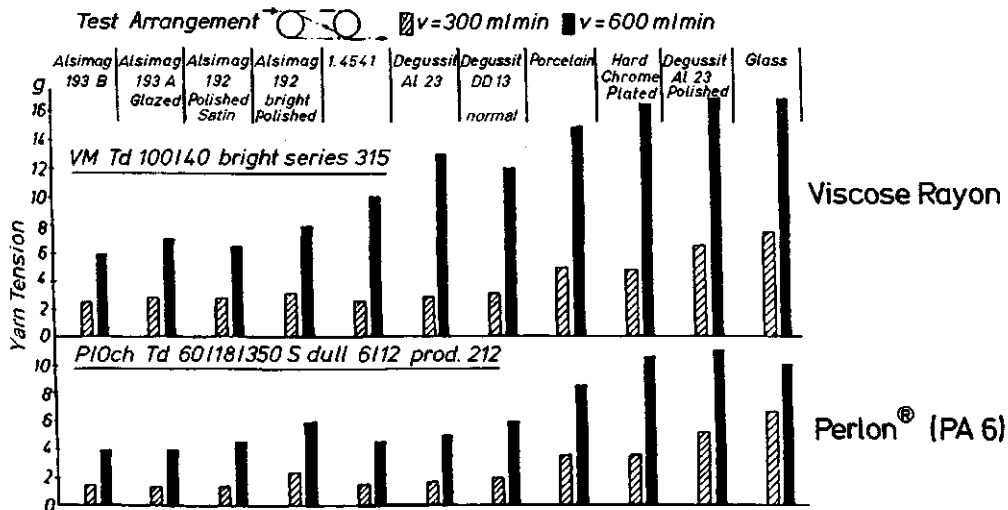
Figure 7.7b   Post-pin yarn tension as a function of pin material at constant angle of wrap [86] (pre-pin tension is low); wrap angle ca. 390° ≈ 6.81 radians. Additional approximate coefficients of friction (measured by the twist separation principle) [85]

Materials	friction coefficient	Materials	friction coefficient
wool/wool		CA/CA (acetate)	0.56
in scale direction, dry	0.11	CLF (Saran)	0.55
against scale direction, dry	0.14	PA 66/PA 66	0.47
against scale direction, wet	0.22	PET/PET	0.58
cotton/cotton	0.22	glass/glass fiber dry	0.28
silk/silk	0.52	fiber with finish	0.18...0.2
CV/CV (rayon)	0.43		
Teflon/hard chrome, matt, static	0.20		
dynamic	0.28		

among others]. As the ceramic guide molds are very expensive, standard guides should be selected, as appropriate, from manufacturers' catalogs. Electrically conductive versions are often available.

The preferred areas of application for the yarn guides shown in Fig. 7.8 are:

(1) yarn aspirator mouthpieces
(2,3,4) traverse guides
(5,7) centering yarn guides for stringing up using an aspirator pistol.
(6) guides for coning- and textile winding machines
(8) comb guides, for many yarns in parallel
(9) roll guides for single yarns or for many wraps, placed after delivery rolls on, e.g., drawtwisters.
(10) yarn assembly- and separator tube and pin guides, e.g., in warping

Figure 7.9 shows typical spin finish applicator guides:

(1) short applicator for low oil pick-up
(2) applicator recommended for POY spinning, 40...ca. 230 dtex
(3) applicator for technical- and BCF yarns

For guides which experience motion (e.g., yarn winder traverse guides), the most important criteria are self-threading ability, guide form (short or protruding) and guide weight, the last-mentioned determining the maximum traverse guide speed (section 4.9.5.2, Fig. 7.10). In these guides, the yarn-bearing Al_2O_3 ceramic (e.g. 2 or 3 in Fig. 7.8) is molded into a polyamide shoe for small guides or is screwed to the shoe for larger guides in order to achieve a smooth gliding motion in the groove of the traverse cam. Often Molycote® [29] is applied to the guide on insertion to improve lubrication (Fig. 7.11).
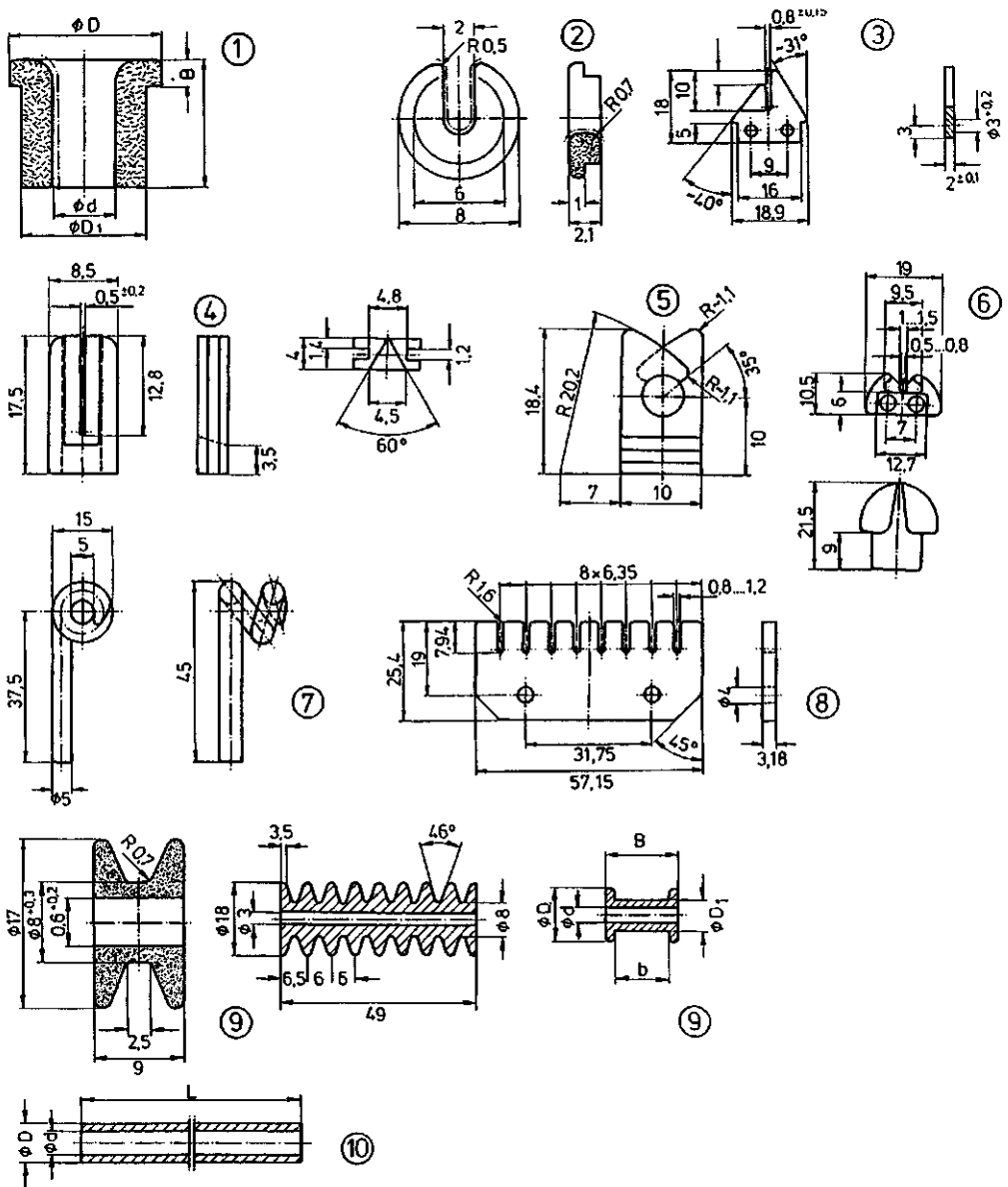
Figure 7.8   Selection of commercially-available yarn guides taken from manufacturers' catalogs [23–26]

1 Eyelet, closed

2 Self-threading eyelet

3 Self-threading traverse guide

4 Slit guide

5 Re-threadable eyelet guide

6 Shoe guide

7 Pigtail guide

8 Comb guide

9 Various roll guides

10 Tube guides, pin guides
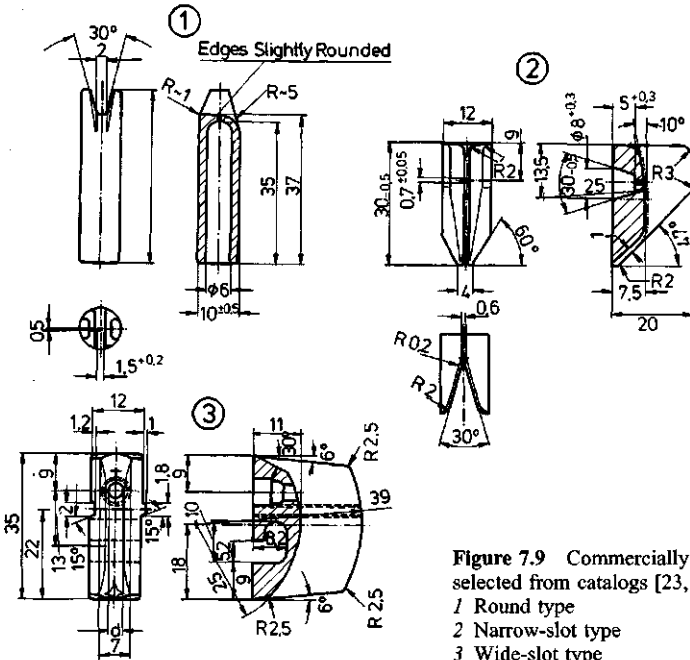
Figure 7.9 Commercially available spin-finish applicators, selected from catalogs [23, 24]
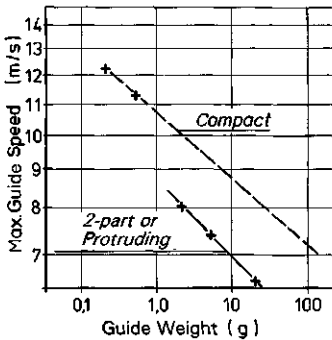*1* Round type
2 Narrow-slot type
3 Wide-slot type

Figure 7.10
Maximum linear traverse speeds of yarn guides in cross-winding (statistical)

In Fig. 7.11, guide (A) is intended for a POY winder [22] and permits a linear guide speed of max. 11 m/s, guide (B) is from a MOY winder with up to 8 m/s traverse speed, guide (C) for a POY winder with up to 11.7 m/s and guide (D), with its protruding guide-bearing arm, for up to 4 m/s linear traverse speed.

Owing to its lever-action tilting effect, guide (B) gives a particularly good edge lay (good sidewalls). An initial rough estimate of the expected traverse guide lifetime can be calculated from the formula: z (lifetime in days) $\approx 100/[\text{m/s}] \times (\text{g})$. The need to change traverse guides quickly necessitates a boat-shaped shoe and an insertion gap in the cam housing rail (Fig. 7.12).

Spin finish applicators are also a type of slit yarn guides in which the spin finish is dosed through a small bore in the applicator body so as to wet the yarn before it contacts the applicator body, and is then kept in contact with the descending finish for a sufficiently long time. Often two opposed spin finish applicators are used when the yarn filament count is high and/or when more uniform finish penetration is required.
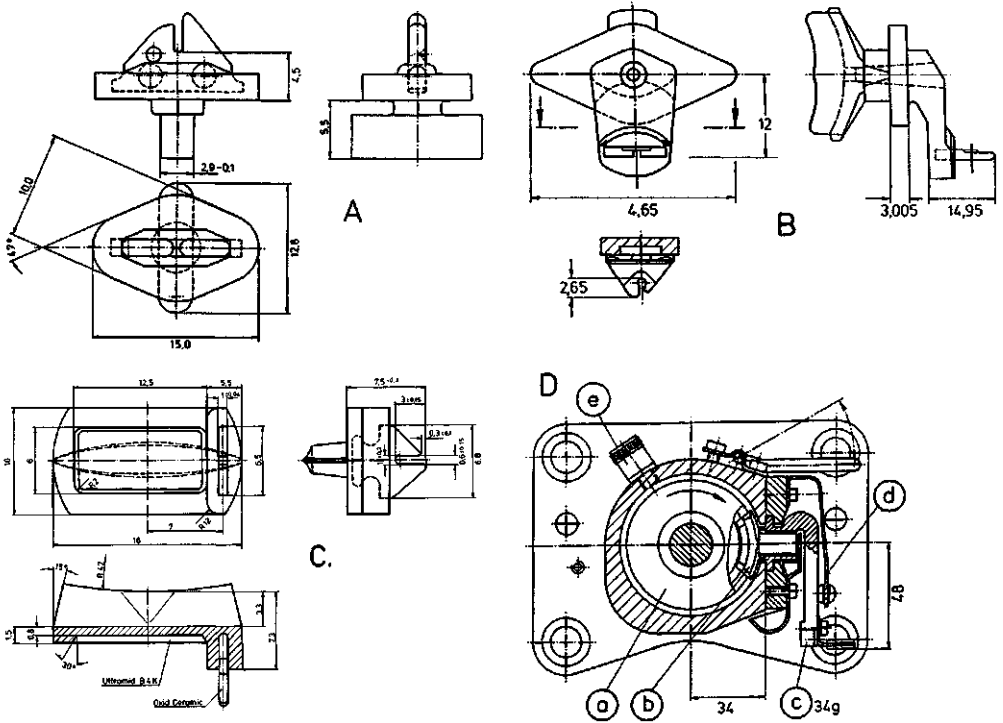
Figure 7.11   Examples of traverse guides
   A) from a high speed winder (up to 6000 m/min) [22]
   B) from a high speed winder (up to 4000 m/min), with tilting acceleration at reversal [31]
   C) from a winder for 6000 m/min [22]
   D) from a 2000 m/min winder, with extended guide-bearing arm and integrated traverse camshaft
         [22]
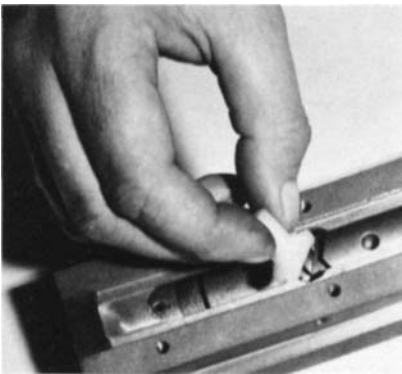   The versions *A*) to *C*) are self-threading

Figure 7.12
Insertion of a traverse guide (B in Fig. 7.11) into the guide rails
and cam groove [31]

As the applicator bores tend to block after a short time, despite the use of single finish pump dosing, a careful daily check is necessary; when required, the bores should be rodded clean using a soft, fine copper wire.

Yarn sensors are also a type of yarn guide, having the function of sensing or signalling whether yarn is travelling past the guide. Here the yarn can run through an eyelet- or slit-guide or over a pin. Because of their importance in automation, yarn sensors are located immediately above the winder traverse
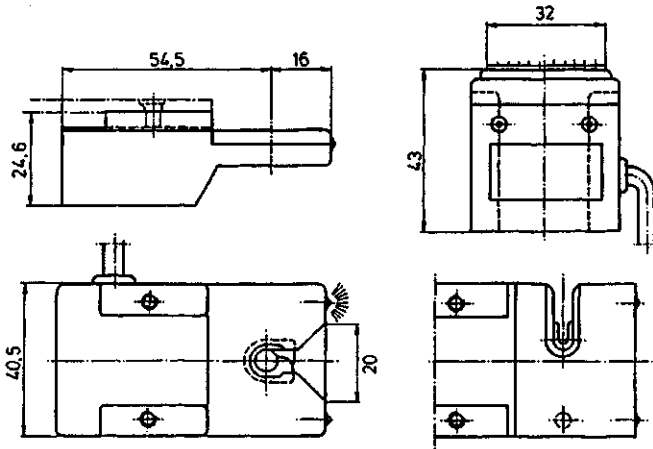
Figure 7.13
Electronic yarn sensors
(contactless) [28]

triangle in order to trigger the required signals at a yarn break (Fig. 7.13). Microswitches having an extended, Al_2O_3-coated lever arm were previously used [27]. These function satisfactorily only up to ca. 1000 m/min; they are nowadays rarely used.

Non-contact yarn sensors can be used as length monitors when producing equilength yarn packages [28]. They can be used, e.g., to automatically initiate a doff after a pre-set time on a revolver winder or to signal the need for corrective action at a yarn break.

7.3   Yarn and Tow Cutters

These cutters are positioned in the yarn path either shortly after the yarn/tow aspirator or before the take-up device, their function being to cut the yarn at a yarn break on receipt of a signal from the yarn presence sensor and to permit the still-running yarn to be aspirated, thereby avoiding yarn wraps and tangles on the machine. The most frequently used types are the anvil cutter for textile yarns (Fig. 7.14) and the scissors cutter for multi-cables or wide cables (Figs. 7.15 to 7.17). Both types are compressed air activated, and cut either simultaneously with the activation of the complementary yarn aspirator, or after a delay of ca. 0.1 s [30].
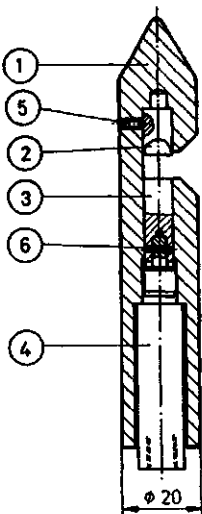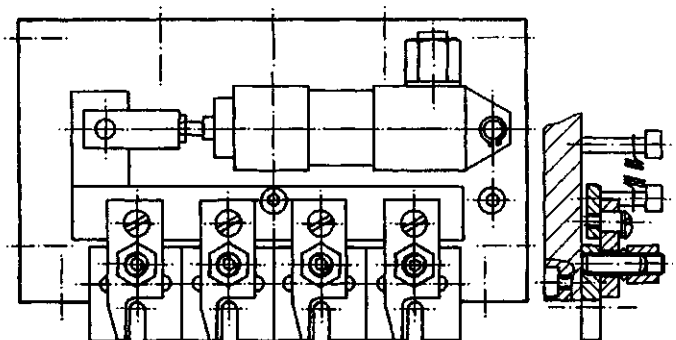

Figure 7.14
Yarn cutter (anvil principle) [22]
1 Housing	*4* Compressed air cylinder
2 Anvil	*5* Clamping screw
3 Percussion knife	*6* Pin

Figure 7.15
Fourfold yarn cutter
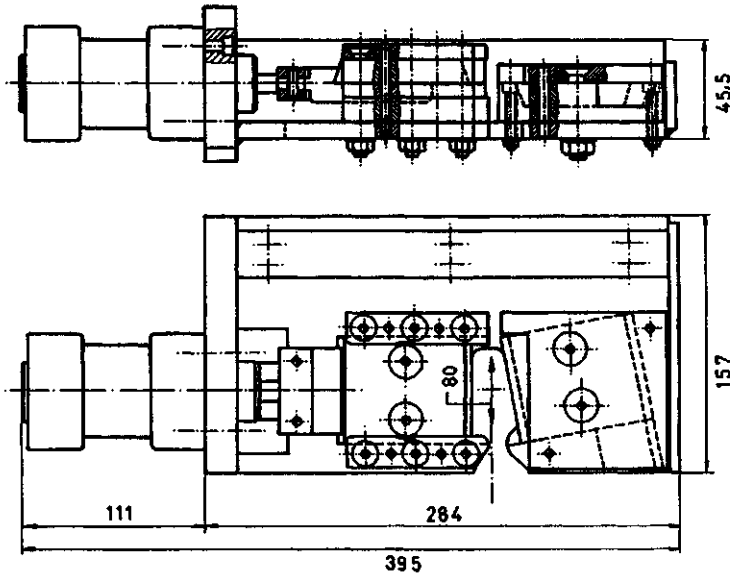(scissors principle) [31]

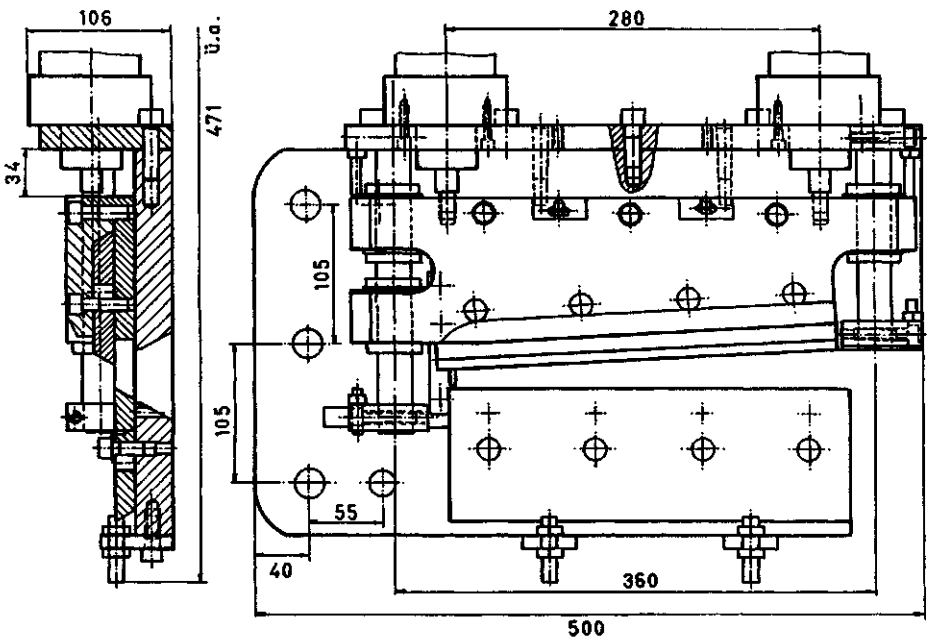**Figure 7.16**
Wide-band cutter [30]

Figure 7.17   Tow cutter [30]

In the scissors cutter, the cutting surface meets the other surface at a small angle in order to spread the cutting forces uniformly across the cable. Such large tow cutters facilitate the stringing up of cables from drawstand to drawstand and can contribute to automation.

7.4   Air Jets

7.4.1   Yarn Aspirator Jets

The relationships given in Section 4.12.5, among others, are valid for yarn aspirators. The most important area of application of aspirators is on the spinning machine, where both machine-mounted and hand-held aspirators are used. Hand aspirators are also used in further-processing machines. The aspirator principle is shown in Fig. 7.18: air flow Q_1 at pressure p enters the inner tube through a slit, thereby aspirating the air flow Q_2 and the yarn (a) through the gun mouthpiece; they emerge at the gun exit (b) together as flow Q_3.

The photograph in Fig. 7.18 shows a typical hand-held aspirator gun [33]. Figure 7.19 shows the aspirator air consumption and the achievable yarn aspiration speeds as a function of compressed air pressure. Further data are given in Table 7.5.

Figure 7.20 shows, as an example, the threading up of 4 ends from a godet (delivery roll) onto 2 winders in double-deck configuration, each winder having 2 yarn packages. The 4 ends are aspirated into the hand gun after the godet, then 2 ends are threaded into the upper winder traverse triangle yarn guides and the remaining 2 ends into the lower winder traverse triangle yarn guides. The 2 upper threadlines are next pulled into the catching grooves of the paper tubes of the upper winder, and the lower threadlines into the grooves of the lower winder paper tubes. On being caught, the threadlines immediately wind onto the tube, thereby breaking the yarn at the aspirator mouthpiece. Both high titer yarns and technical yarns must, however, be cut during donning (stringing up).

The exhaust air—and waste yarn aspirator hoses must be wide enough, must be electrically conductive and need to be earthed.

Similar aspirators, one per threadline, can be built into the spinning take-up machine. It is also possible to fit an aspirator at the bottom of each quench tube to suck away spun yarn waste at start-up. In this case, the yarn take-up speed is irrelevant (Fig. 7.21 [22]).

The yarn tension induced by the aspirator should be >10 cN/yarn for textile yarns and >30 cN/yarn for technical and carpet yarns, as the lick-back ("sticking to roll") tension of godets is of the order of $8 \ldots 10$ cN/yarn.
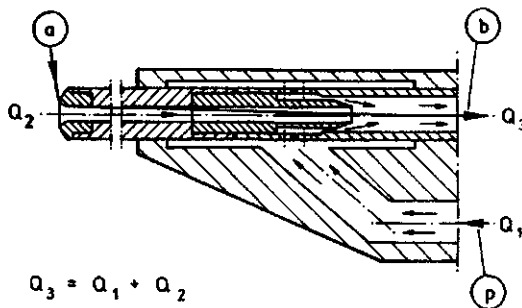

$$Q_3 = Q_1 + Q_2$$

Figure 7.18
Schematic section of a single-stage hand-held yarn aspirator (gun) having a ring air injector [33]
$Q_1 =$ compressed air
$Q_2 =$ air aspirated with yarn
$Q_3 =$ yarn transport air
$Q_3 = Q_2 + Q_1$
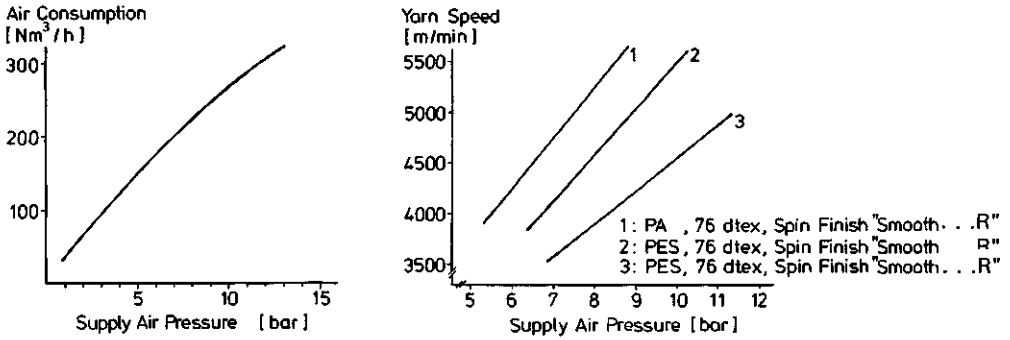a) mouthpiece (exchangeable, made from sintered Al_2O_3)

Figure 7.19   Air consumption of the hand aspirator shown in Fig. 7.18 as a function of inlet pressure (left) and achievable yarn speed for various yarns (right) [33]

Table 7.5   Technical Details of Yarn Aspirator Jets

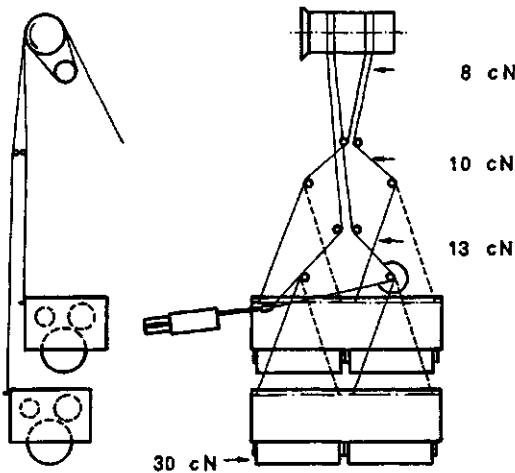| Velocity	Titer	Process	Yarn type	Aspirator nozzle diameter D	Air pressure	Air consumption	
m/min	dtex			mm	bar	Nm³/h	
≤2000	≤2000	Turns/*m*	Textile, techn., carpet yarn	10	6	65	Fixed to machine
	≤20 000		tow	15	6	150	
≤1700	≤80 000	Fiber	tow	20	6	500	
2000	≤1000		Textile	7	6	100	
3500					6	235	
	≤3000	BCF, technical	POY, FOY	7			
5500					16	300	Hand gun
3500			POY, FOY		6	340	
	(4...8)	POY		7			
	× 250)	FOY	Also from				
6000			godets (rolls)		10	540	

Figure 7.20
Threading-up of a 4-fold, double deck yarn take-up machine using a hand aspirator (measured yarn tensions are given) [33]
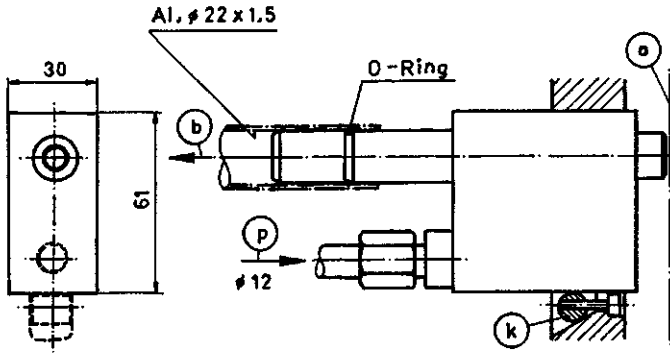
Figure 7.21
Machine-mounted aspirator [22]
a) Thread to be aspirated
b) Aspirated yarn to waste, after cutting
p) Compressed air connection (6 bar)
k) Clamping device

In order to reduce the very high air consumption (particularly for speeds >5500 m/min), an aspirator pistol has been developed in which the yarn is taken up inside a centrifuge and is then taken away under the conditions: $\approx 200\,\text{Nm}^3/\text{yarn} \times 7$ bar and 100 cN/yarn [22].

7.4.2   Intermingling Jets (Tangling Jets)

Intermingling has proved to be a good and cost-effective substitute for the previously widely-used twist or protective twist of 10 ... 20 turns/m. Intermingling is also carried out after texturizing on draw-texturized or BCF yarns. Both open (Fig. 7.22) and closable (Fig. 7.23) tangling jets are used; in both cases they can be threaded up using a hand aspirator.

In the case of closed or closable intermingling jets, the air stream is directed onto the yarn (almost) perpendicularly and intermingles or tangles the individual filaments to form a distinct knot. This system works well up to ca. 1200 m/min.

The open system [37] incorporates an impact plate, and can be threaded up with a hand aspirator at speeds above 4000 m/min. Air consumption is given in Fig. 7.22. The technical data given in Table 7.6 [33] is generally valid. Additional intermingling jets—also for higher titer ranges—are made by [33, 38–40]; Figure 7.24 shows an example of such a jet. Reference [39] gives compressed air requirements.

Two yarn ends can also be joined by means of intermingling (Fig. 7.25); previously they were knotted together. The two ends to be spliced together are laid slightly diagonally in the splicer, the free ends are cut off and the compressed air is switched on. After splicing, the yarn is removed. The size of a hand-held splicer can be seen in the photograph in Fig. 7.25.
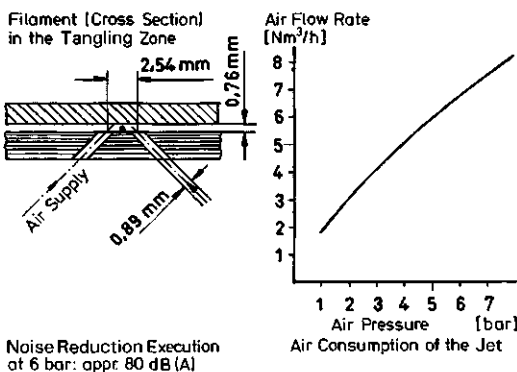

Figure 7.22   Intermingling jet [33] incorporating a noise-reduction principle (ca. 80 dB at 6 bar), air consumption at different pressures and a photograph of it mounted on a drawtwister
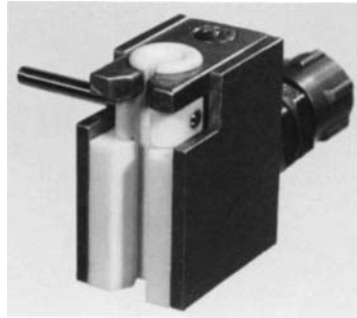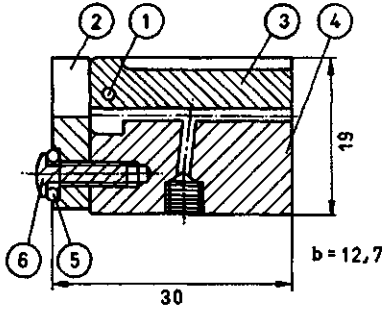
Figure 7.23   Intermingling jet: openable for threading up, closed during operation (19 mm deep ×
12.5/28 mm wide × 30.2 mm high) [38]
   1 Stainless steel pin   *4* Plate, 1.4301
   2 Ceramic yarn guide, swivels to open   *5* O-ring
   3 Ceramic insert   *6* Rotational axis for item 2
   Technical data:

Jet inside diam.		titer range	compressed air consumption at				
inches	mm	den	kg/cm^2	1.4	2.1	2.75	3.4	4.1
0.1	2.5	250...600		1.4	2.1	2.75	3.4	4.1
0.06	1.5	110...250	Nm^3/h	2.4	3.3	3.9	4.6	5.3
0.05	1.3	70...110					
0.04	1.0	30...90	Nm^3/h	0.7	0.9	1.1	1.3
0.03	0.8	15...70					

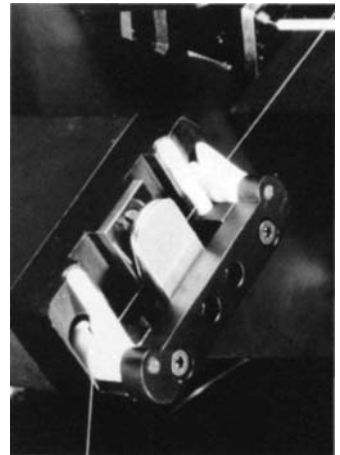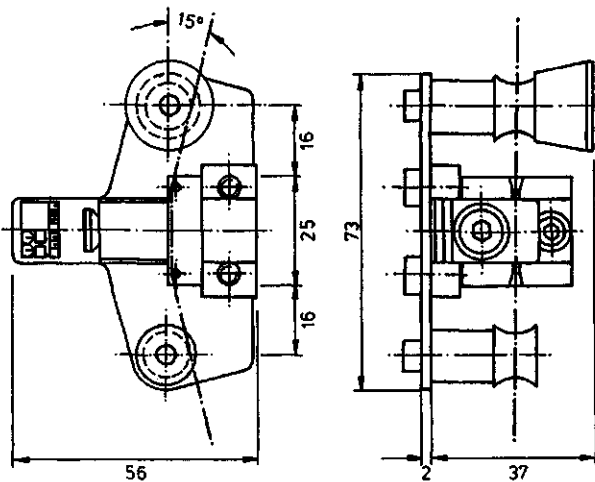**Figure 7.24**   Intermingling jet for 200...3000 dtex [40], drawing and installation.
   Compressed air requirements:
   — pressure deviation: max. 0.1 bar
   — temperature: 25 °C ± 5 °C
   — RH: 40%
   — residual oil content: ≤ 0.2 ppm (ideally, oil-free and chemically neutral)
   — contamination: free of abrasive particles
   — particle size > 0.2 µm: 100% to be removed (1 ppm ≈ 1 mg/m³)

Table 7.6   Technical Details (Average Values) of Commercially-Available
Intermingling Jets [38, 39, 40, Standardized]

Supply pressure	$3\ldots4$ bar for textile ($20\ldots220$ dtex)
	$4\ldots8$ bar for BCF (≤2500 dtex)
Supply air pipe diameter	(2.26 ± 0.05) [mm]
Yarn transport pipe diameter	$(0.006\pm0.003)\cdot$ dtex [mm]
Air consumption	$(0.0039\pm0.001\cdot$ p (bar) $\cdot$ dtex [Nm^3/h]
Entanglements/m	$20\ldots60$ for textile yarns
	$8\ldots20$ for BCF
	$5\ldots15$ for high speed and ceramic insert
BCF heat set yarn [39]	for up to $5500\ldots12000$ dtex
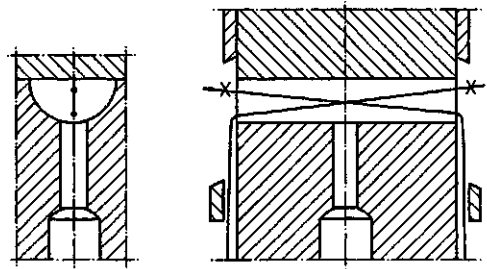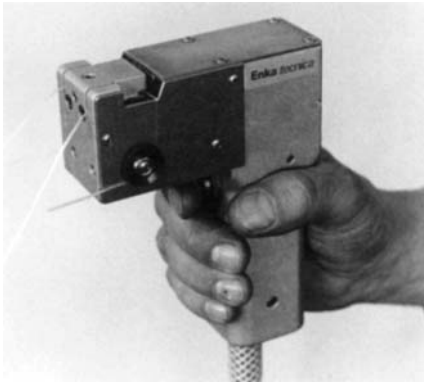
Figure 7.25   Hand splicer—used to join two yarn ends by intermingling: principle and photograph [33]

7.5   Rotating Cylinders (Godets, Yarn Bobbins, etc.)

A rotating cylinder of finite length drags an air boundary layer with it, and therefore requires a torque of $M_\mathrm{D} = 0.087\,\mathrm{Re}^{-0.2}\,b\cdot d^2\,(\rho\cdot v^2/2)$ [41] to maintain its rotational speed.

From this torque, the drive power required can be calculated:

$$N\,[\mathrm{kW}] = 0.102\,b\cdot d^2\cdot v^{1.125},$$

with $b=$ roll length [m], $d=$ roll diameter [m] and $v=$ circumferential speed [m/s]. The factor (for running in air) and the exponent may need to be adjusted according to experimental results. A friction drive roll of 150 mm diameter × 900 mm long running at 6000 m/min would therefore require a power input of 2.448 kW; its corresponding paper tube of 104 mm OD approximately 1.622 kW extra. At full package size (420 mm diameter), this would increase to 5.804 kW; the energy transfer to the package occurs through friction. The total power required therefore becomes 7.452 kW at 12732 r/min ($=212.2$ Hz) friction roll speed, which corresponds to 1.756 kW at 50 Hz. The corresponding calculation for a chuck and empty tubes gives 0.97 kW. The larger value must be used for sizing the motor.

To the above power requirement must be added the power to overcome bearing friction (20%) and yarn tension (8–10%), as the example in Fig. 7.26 shows.

The power transmitted from the winder friction drive roll to the spun yarn package appears in the form of frictional heat, which must be removed by the air conditioning, so that neither the friction roll nor
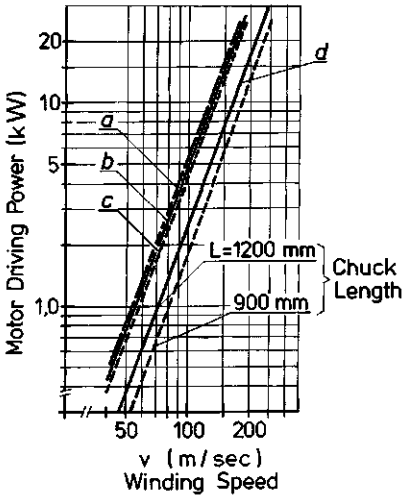
Figure 7.26
Measured and calculated friction drive roll motor power
without (calculated for 2 chuck lengths) and with yarn
packages, c) without and b) with bearing friction and
a) including yarn winding tension [42]

the yarn package exceeds the glass temperature. This overheating effect has, e.g., led to cases where PA
66 bobbins have become unacceptably deformed, and the only solution then was to use a spindle
drivewinder.

7.6   Inclined Rolls

A yarn running on a roll or godet always leaves the roll normal to the roll axis [43]; this makes it possible,
by using two mutually-inclined rotating rolls, to transport the yarn sideways wrap after wrap. There are
three possible ways of doing this:

- As Nelson rolls, first used on a continuous v—scose spinning machine ([44, 45], Fig 4.352), with a
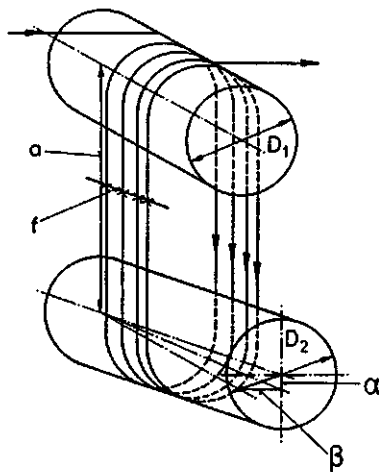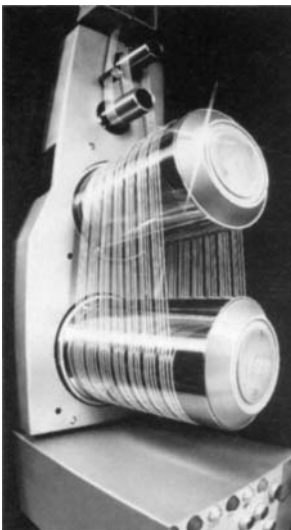 godet center to center distance of a $\gg$D—the most widely used system today. The sideways

Figure 7.27
Yarn transport and
accumulation by means of
two mutually-inclined rolls
(4-fold) [17]

displacement of the threadline (pitch) per half wrap is, according to Fig. 7.27 (see comparative photograph), given by:

$$f \approx a \tan \alpha + b \tan \beta,$$

where α is the angle in the connecting plane and β is the angle perpendicular to this. When $\beta = 0$, the roll to roll distance becomes increasingly smaller, and the yarn instability increasingly worse (unless the yarn shrinks during transport). An effective setting is $\alpha \approx 0.1 \ \beta$. Table 7.7 gives guidance values for the yarn sideways displacement f (pitch). If $D_2 \ll D_1$, (e.g., a godet fitted with a separator roll), then:

$$f \approx a \tan \alpha + \frac{D}{2} \tan \beta.$$

Table 7.7 also gives guidance values for this case.

Table 7.7   Yarn Pitch on Inclined Godets (Rolls) (See Fig. 7.27 for a, D, f)

2 rolls, each of diameter D [mm]	$a - D = 120$	$a - D = 1000$	1 godet with idler roll
120	7.54	12.15	4.09
150	9.27	13.88	4.95
190	11.58	16.19	6.10
220	13.31	17.92	7.00
			$(a - D = 120)$
500	29.45	34.06	

- The Boos reel [46], which has pins placed on 2 circles. The pins are located alternately on two eccentrically-running circles.
- The spooling reel (Fig. 4.353), in which the pins, axially protruding as above, additionally move forwards and then backwards after meshing with the pins of the second roll [47].

The latter two systems are practically obsolete.

7.7   Melt and Solution Viscosity

These two viscosities and their variation coefficients are important production variables. Solution viscosity characterizes the polymer uniformity and enables—through given relationships—calculation of the molecular weight. Melt viscosity determines the polymer flow through the spinneret capillaries (bores) and its uniformity, namely the titer uniformity; temperature deviations, shear stress and molecular weight distribution also play a role.

7.7.1   Melt Viscosity

The capillary throughput per hole can be calculated from the relation: $Q_1 = \pi D^4 p / 128 \eta L$ [48]. If one equips the measuring apparatus with a flow-measuring pipe or gap, one can—after taking into account the Hagenbach correction [49], among others—obtain the melt viscosity from the pressure drop Δp and the throughput Q_1, at constant temperature, and evaluate it using a microprocessor. Figure 7.28 shows results obtained from such a capillary melt viscosimeter [50] for a series of PET polymer samples having a range of viscosity CV's. Such an instrument can be so sensitively set that even the polymer pump rotation and pump gear teeth can be detected (Fig. 4.159). By switching off the temperature compensation, the effect of temperature variations on the Uster value can be determined by in-line measurements, by spinning with- and without temperature compensation.

In another method (Couette principle), two concentric rotating cylinders are used to determine melt viscosity; the result is as exact as the above method.
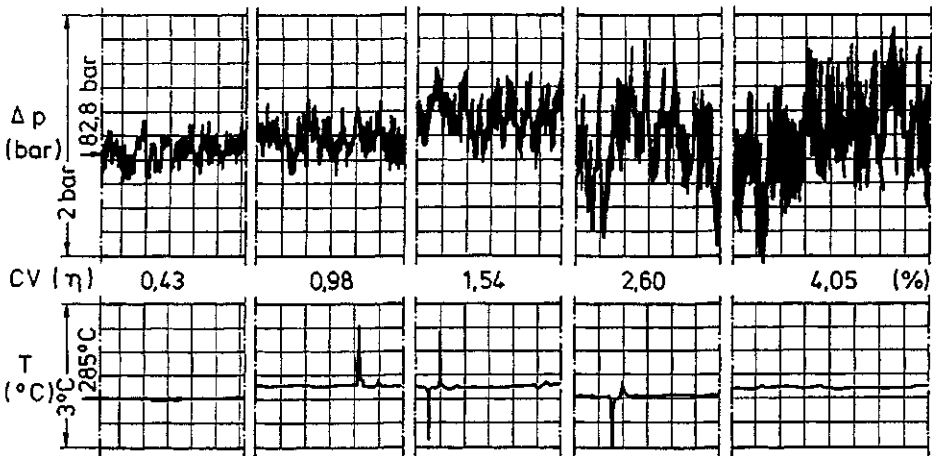
Figure 7.28   Pressure and temperature recordings of polymer melt flow using a Fourné Visco-Data-Processor, and a microprocessor evaluation of viscosity deviations [30] (^ = time signal)

The melt viscosity temperature dependence can be experimentally determined using the same two methods above. It can also be calculated from:

$$\eta = A \cdot e^{E/RT} (= K \cdot Y^{2.5}),$$ where A and E are molecular weight-dependent constants.

7.7.2   Solution Viscosity

The determination of solution viscosity is important, as it enables (via theoretical relationships) the calculation of the molecular weight of the polymer and its variation, from which its spinnability can be judged and the effect on the resulting properties assessed. For historical and geographical reasons, many different solvents, methods and definitions are still used in solution viscometry. Section 10.2 summarizes some of these, and gives constants and nomograms for conversion from one system to another.

The Ubbelohde viscosimeter, in an accurately controlled temperature bath (Fig. 7.29; section 10.2), is used to determine solution relative viscosity. The run-through times of the polymer solution and the pure solvent are measured, and the relative viscosity is calculated from:

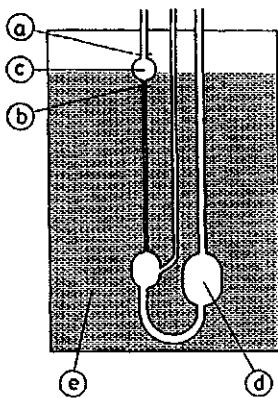$$\eta_{\text{rel}} = \eta/\eta_0 = t\rho/t_0\rho_0 \approx t/t_0,$$

Figure 7.29
Principle of Ubbelohde solution viscosimeter
a), b) Calibration marks
c)   Volume for determination
d)   Solution storage
e)   Constant temperature bath

where t = drainage time, ρ = density and "0" designates the solvent. In order to obtain a desired accuracy in η_{rel}, the measurement conditions given in Table 7.8 [77, 52] must be strictly adhered to. As the theoretically-required extrapolation of the polymer concentration to the limit $c \to 0$ is very difficult, in practice certain agreed-on concentrations are used (see also Table 7.8).

Table 7.8   Accuracy of Solution Viscometry [52]

Desired accuracy in η_{rel}	± 1	± 0.5	± 0.1	%
Required temperature constancy	± 0.1	± 0.05	± 0.01	°C
Allowable measurement error	± 0.33	± 0.17	± 0.03	%
Measurement time	250...100	330...100	650...100	s

As it is frequently used, the method has been automated and the test results are calculated using a microprocessor, which takes into account the Hagenbach correction (DIN 51512, 53728). Up to 12 Ubbelohde viscosimeters are placed in one bath; the entire process of sucking up solution, drainage, timing and calculation has been automated [83].

The origins of PP lie in the plastic industry, and a different system of measuring viscosity was therefore adopted, the so-called MFI (melt flow index) method (Section 2.4.1.1). To date, only experimental relationships exist between MFI and η_{rel} or $[\eta]$ (e.g., Fig. 2.69). In the MFI method, melt at an exactly-defined temperature is forced through a defined nozzle under a defined pressure, and the throughput in g per 10 min is measured to give the MFI index. Table 7.9 gives standard test conditions. The most frequently used MFI test is carried out at 2.16 kg load and 230 °C, the result being quoted as $\text{MFI}_{230,\ 2.16}$. Figure 7.30 shows the principle of a MFI tester [84].

The deviation from the average solution viscosity characterizes the uniformity (narrow molecular weight distribution) of polymer from a batch. Here one should measure, e.g., 6 samples from each charge for all n charges, and from these results calculate the batch average and deviation (Δ). These Δ values should not exceed the experience values in the table below. It should, however, be noted that the solution viscosity can decrease by 0.02...0.05 as a result of thermal degradation, etc., during melt spinning.

Allowed deviations of rel. viscosities

Polymer	PA	PET	PP
For production of	$\eta_{rel}\ (H_2SO_4)\pm$	$[\eta]\pm$	MFI$\pm$
Microfibers	0.005	0.005	
Tire cord	0.01	0.01	
High tenacity (technical) yarns	0.015	0.015	0.4
Textile yarns	0.02	0.02	0.5
Staple fibers: HMHT		0.015	
standard	0.03	0.02	0.5
ex waste polymer	0.06	0.05	1.0

7.7.3   Molecular Weight, Polymerization Degree, etc.

The theoretical relationships between solution viscosity, molecular weight, polymerization degree, chain length distribution and melt viscosity are given in [54, page 197; 55, page 193 and 51, page 394] in sufficient detail for our purpose here. As these relationships are of a very theoretical and experimental nature and are not confirmed in the general literature, only those results and constants which are frequently used in practice are given below, without comment on their reliability or exactness.

Table 7.9   Test Conditions
for MFI Determination

Load kg	Temperature °C
1.2	190
2.16	230*
3.8 5.0 10.8 21.6	± 0.5

*mainly for PP
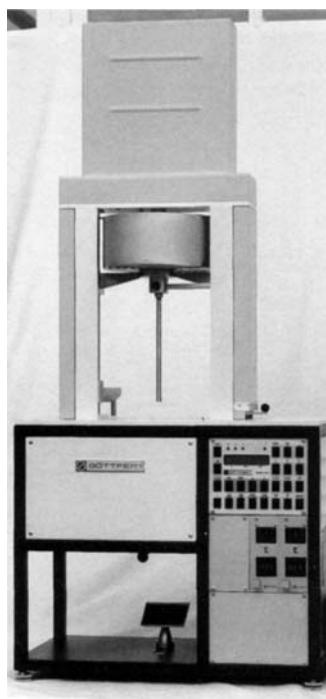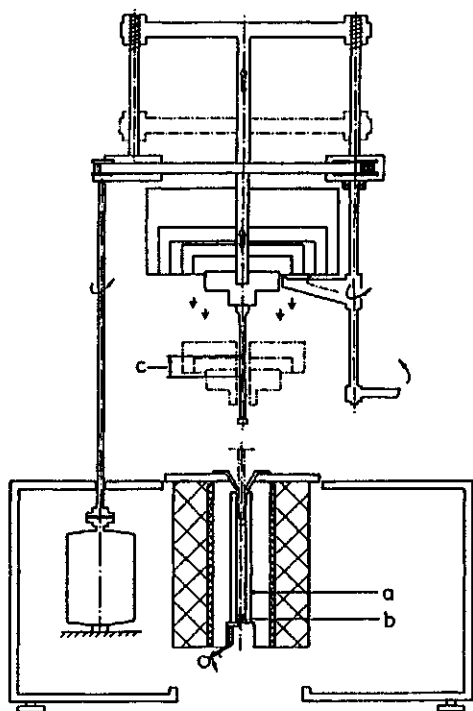
Figure 7.30   MFI measuring apparatus [84], schematic and execution with microprocessor evaluation

The Mark-Houwink-Staudinger equation applies to homologous polymer macromolecules of ≥ 100 monomer units:

$$\bar{\eta}_{rel} = K_\eta \bar{M}^\alpha, \text{ where}$$

η_{rel} = average relative solution viscosity

K_η, α = polymer and solvent-specific constants ($0.5 < \alpha \leq 1$, mainly $0.65\ldots0.8$)

$\bar{M}$ = average molecular weight.

Table 7.10   Effect of Solvent Temperature on K_η and α

Polymer	Solvent	Measurement temperature °C	$K_\eta \cdot 10^4$ dl/g	α
Polyacrylonitrile (PAN)	Dimethylformamide	20	1.77	0.78
	Dimethylformamide plus 0.9 g/l $NaNO_3$	25	2.10	0.74
Polyamide 6 (PA 6)	Trifluoroethanol	25	5.36	0.75
	Aqueous formic acid (85%)	25	2.36	0.82
Polyamide 66 (PA 66)	Aqueous formic acid (90%)	25	3.53	0.786
Polyamide 12 (PA 12)	Hexa flouroisopropylalcohol	25	8.43	0.68
	m-Cresol	25	6.21	0.73
Polycarbonate (PC)	Methylenechloride	25	1.19	0.80
Polyethylene high	Tetralin	120	3.8	0.73
density (HDPE)	α-Chloronaphthalene	127	6.9	0.67
Polyethylene terephthalate	Trifluoroacetic acid	30	4.33	0.68
	Phenol/Tetrachloroethane (3/5 Vol)	30	2.29	0.73
Polypropylene (PP)	Decalin	135	1.10	0.80
Polystyrene (PS)	Toluene	25	1.05	0.73
Polyvinylalcohol (PVA)	Water	30	4.28	0.64
Polyvinylchloride (PVC)	Cyclohexanone	25	1.38	0.78
	Tetrahydrofuran	30	6.38	0.65

Table 7.10 gives the effect of solvent temperature on K_η and α.

From the Mark-Houwink-Staudinger equation, simplified formulas can be derived (DP = degree of polymerization):

for PA 6, $\overline{DP} \approx 100\,(\overline{\eta}_{rel} - 1)$, or $\overline{M} \approx 11300\,(\overline{\eta}_{rel} - 1)$,
with η_{rel} measured using n-H_2SO_4 at 20 °C

for PET, $\overline{DP} \approx 520\,(\eta_{rel} - 10.5)$, or $M \approx 10^5\,(\eta_{rel} - 1.05)$,
with η_{rel} measured using tricresol (0.5 g/100 ml) at 20 °C.

The chain length distribution (molecular weight distribution, polydispersity) can be defined by [54]:

$$U = \overline{M}_w/\overline{M}_n - 1,$$

with $\overline{M}_w$ = weight average molecular weight and $\overline{M}_n$ = number average molecular weight.

For very uniform products, $\overline{M}_w = \overline{M}_n$, i.e., U = 0 and for non-uniform products $\overline{M}_w = 2\,\overline{M}_n$, i.e., U = 1. The accuracy cannot be better than the sum of errors in $\overline{M}_w$ and $\overline{M}_n$.

The dependence of melt viscosity η_m on molecular weight and temperature can be empirically expressed by [78]:

$$\log \eta_m = A + B \cdot \overline{M}_w^{0.5} + \frac{C}{T},$$

with A, B and C = constants for a given polymer and T = absolute temperature [°K].

According to another investigation, $\eta_m = K \cdot \overline{M}^{3.5}$. Numerous evaluations of results show a deviation of up to ± 8%.

7.8   Uster Uniformity Testing [57, 58]

In this test, the mass distribution along the length of a yarn is measured, registered and evaluated, enabling one to infer certain properties, and—with additional test equipment—to explain the causes of defective production at fiber spinning and further processing. Test equipment made before 1987 could detect titer deviations down to 0.4%; newer equipment is sensitive down to 0.1%.

The measurement principle is as follows: a well-conditioned yarn runs with a defined speed through a capacitative field of defined length. Mass deviations in throughput change the field; this will be recorded and evaluated. It is essential that the yarn is well conditioned and that the spin finish application is uniform, as these factors affect the measurements. After zero suppression and scale adjustment, the deviations are amplified and recorded on a high speed chart recorder, giving the Uster diagram. The microprocessor evaluation gives, in addition to the Uster value, the frequency and position of the periodicity. According to Fig. 7.31, the coefficient of variation is given by $CV = S/\overline{X}$ [58], with S = standard deviation and $\overline{X}$ = average value of the measurement ($\times 100$ to give %). For a normal distribution, $U = \sqrt{2/\pi}\, CV \approx 0.8\, CV$, where U is the average deviation. The deviation for a non-normal distribution is small.
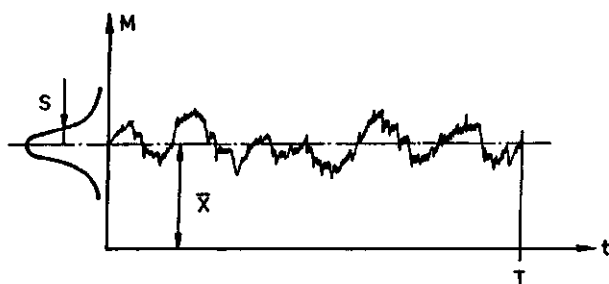

Figure 7.31
Evaluation of average titer, standard deviation and coefficient of variation

In order to use or evaluate the Uster diagram, the following information is needed:

- all yarn data: material, nominal titer, filament count, spinning position or processing position, yarn speed, draw ratio (if required), etc.
- for machine-related effects: all relevant machine data, starting with, e.g., extruder rpm, and including spinning pump type, -size and -speed, temperatures and pressure, quench air velocity, spin finish, as well as mechanically-related data such as godet speed and -diameter, winder take-up speed, package size, friction drum diameter and rotational speed, traverse double strokes and stroke length, yarn tension—and, if possible—yarn tension variations, etc.
- all test/apparatus data: diagram scale, paper speed, yarn speed and possibly false twist insertion.
- if the yarn has been further processed: particularly draw ratio, temperatures, machine position, godet diameters and rotational speeds, separator roll data, etc.

The evaluation, particularly concerning the influences of machine components and operating conditions, requires experience, as can be seen from Fig. 7.32 A to G, which form a series of measurement results related to particular effects, chiefly those of traverse, unround spin bobbins and quench air turbulence. The defective spinning pump (the 420 m periodicity can only be established by measurement and calculation) is an exception. (The test apparatus used here could not measure periodicities of >40 m).

Zellweger, Uster, Switzerland have produced an evaluation scheme for similar, periodic defects; use of this diagram is recommended [60] (Fig. 7.33).

In an investigation at a production site, Fourné [81] investigated the effect of individual process parameters on the Uster value; results are given in Table 7.11, and show that 2/3 of the Uster variation could be explained in terms of mechanical effects between the spinneret and the spin bobbins.

Figure 7.32   Typical Uster diagrams [57–60]
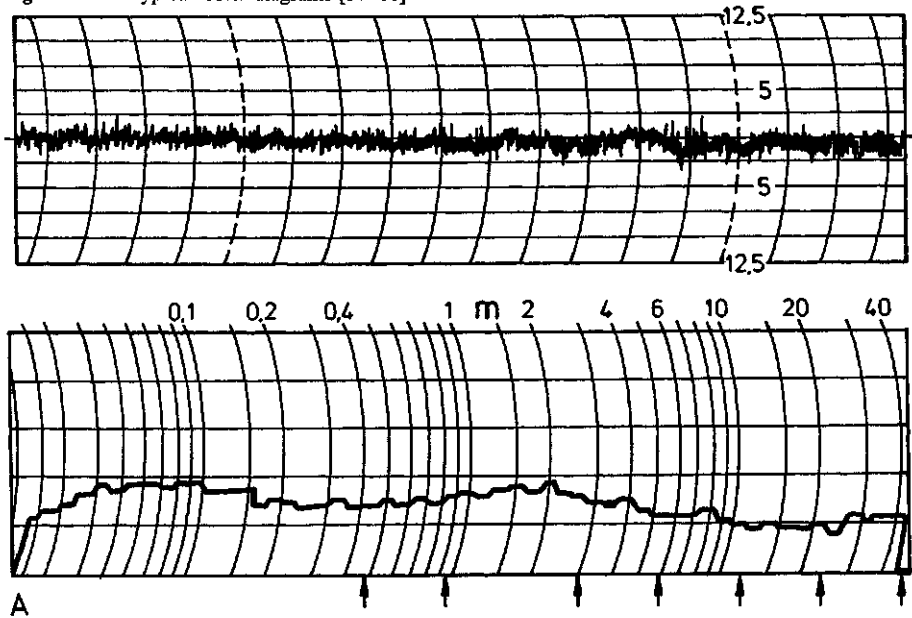
A

Example	Material/Titer Form	CV %	Comments
A	PA66-22f7 drawn cops	0.4	good; no distinct maxima in diagram
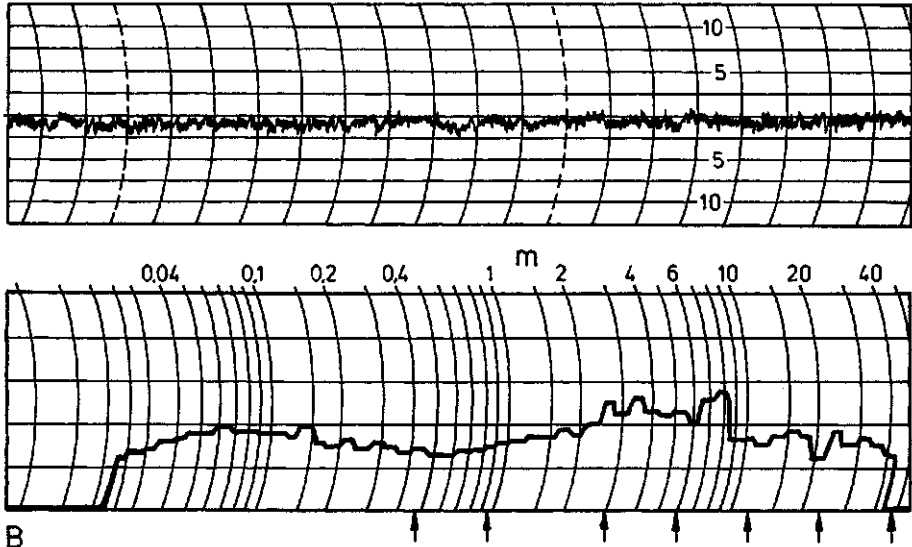
B

Example	Material/Titer Form	CV %	Comments
B	PET-84f16Z	0.5	Still good; periodicity between 2.8 and 8 m: transverse effect
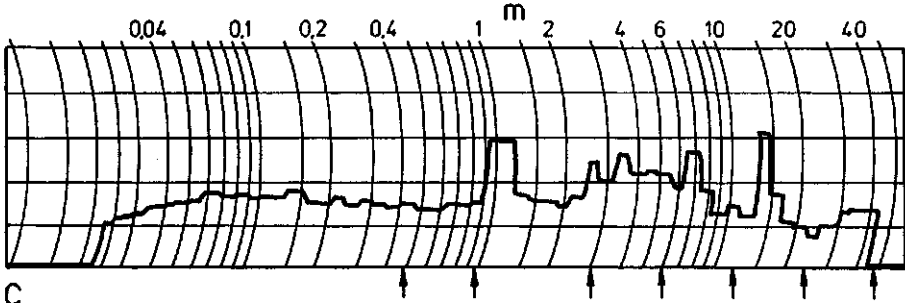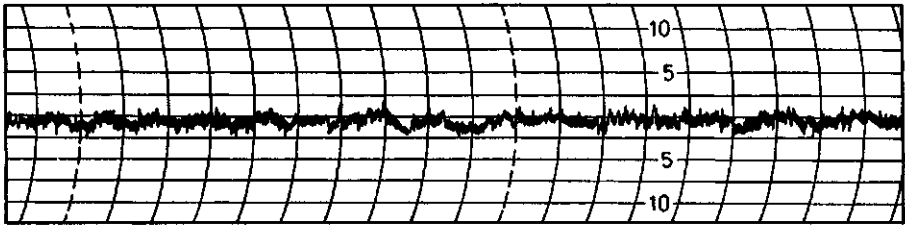
Example	Material/Titer Form	CV %	Comments
C	PET-84f16Z	0.6	No longer good; periodicity at 1–1.3, 2.6, 3.6, (4.8), 7, 14 m could be traverse effects (dominant period and multiples); the 7 m period could also be caused by out-of-round bobbins
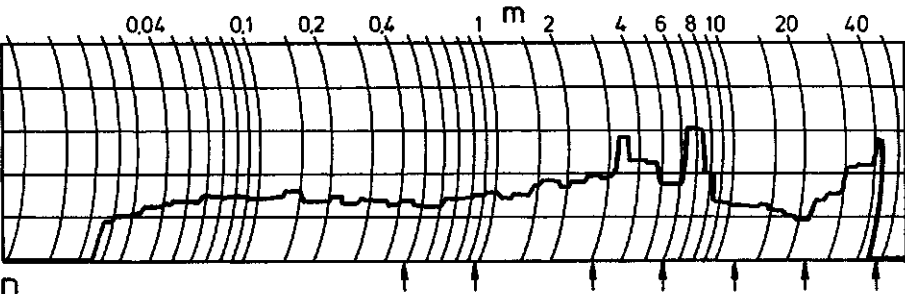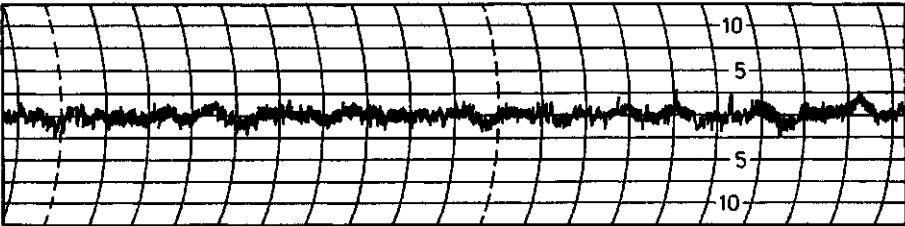
Example	Material/Titer Form	CV %	Comments
D	PET-84f16Z	0.68	Still uniform. Periodicity at 3.5 and 7 ($= 2 \times 3.5$) m: traverse effects. Periodicity at 30–38 m and ≈ 40 m: quench air effects
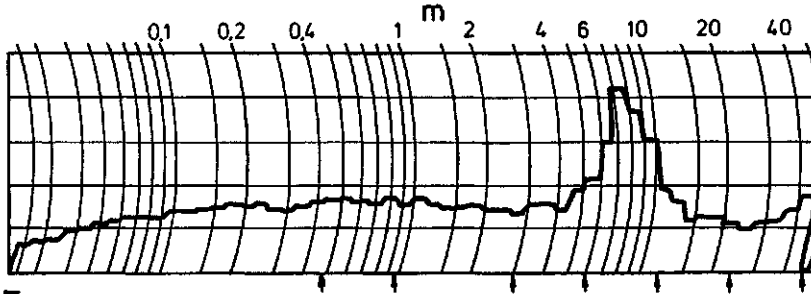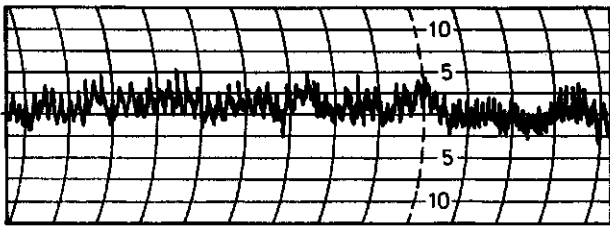
E

Example	Material/Titer Form	CV %	Comments
E	PA66-22f7Z	2	Faulty traverse showing ca. 7 m periodicity, broadened to 5–12 m by wobbling. Periodicity ≈ 40 m: quench air effect
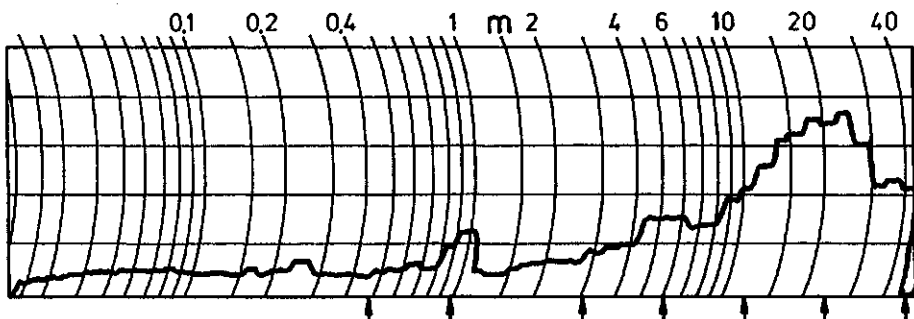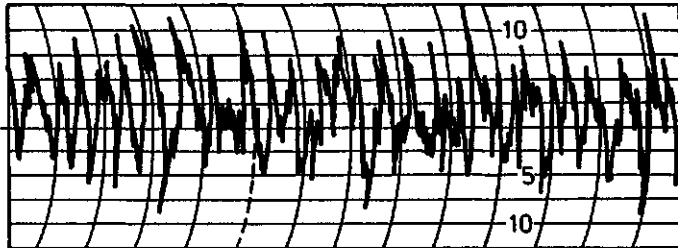
F

Example	Material/Titer Form	CV %	Comments
F	PA66-17f7	5.87	Periodicity of 1 m comes from package circumference, but is unimportant relative to periodicity of 10–40 m: strongly turbulent quench air flow
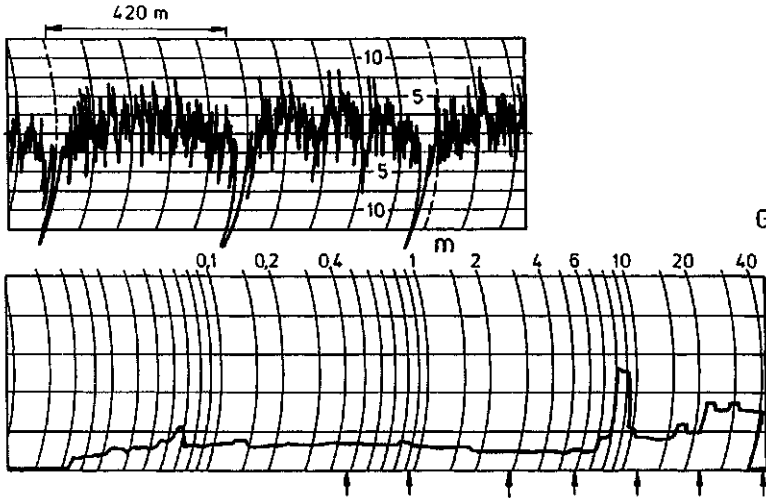
Example	Material/Titer Form	CV %	Comments
G	PET 55f24	3.72	Periodicity 8–9 m: spin bobbins running out-of-round. Periodicity 25–40 m: quench. Periodicity ≥ 420 m (calculated from distances of maxima): defective spinning gear pump

Figure 7.33   Wavelength ranges, evident in Uster diagrams, which can be attributed to machine defects [58, 60]

Spinning machine

Material	Polymide 66
Final titer	$T_E = $ dtex 110f34
Spinning pump throughput per rev	$F_P = 2.4$ g
Production speed	$V_P = 90$-m/min
Winder tube outside diameter	$d_A = 11$ cm
Winder stroke	25 cm
Max. spun package diameter	$d_W = 40$ cm
Traverse double strokes	$H_D = 340$ min^{-1}
Godet (roll) diameter	$d_G = 12$ cm

Required draw ratio at draw-twisting
(see fig above) RV = 3.2

Titer of undrawn yarn $T = R_V \cdot T_E = 3.2 . 110 = 352$ dtex
Required throughput per minute $F_{tot} = T \cdot _V{}^P . 10^{-3} = 25,3.900.10^{-3} = 31.68$ g

Draw ratio of man-made fibers as a function of spinning speed

A: Draw ratio
B: Spinning speed (m/min)
1: Polyester
2: Polymide 66
3: Polymide 6

Draw-twister
Ring rail stroke: empty tubes
Ring rail stroke: full packages
Godet (draw roll) diameter
Production speed

Figure 7.33   *(continued)*

	Cause	Calculation of wavelength range	
Spinning machine	Spinning pump period, measured on spun yarn	$\lambda_1 = \dfrac{v_P \cdot F_P}{F_{tot}} = \dfrac{900 \cdot 2{,}4}{31.68} = 68.18 \text{ m}$	
	Spinning pump period, measured on drawn yarn	$\lambda_2 = R_V \cdot \lambda_1 = 3.2 \cdot 68.18 = 218.2 \text{ m}$	
	Eccentric spun package, at spun package start	$\lambda_3 = d_A \cdot \pi = 11 \cdot 3.14 = 34.5 \text{ cm}$	
	Same fault, measured on drawn yarn (cops)	$\lambda_4 = R_V \cdot \lambda_3 = 3.2 \cdot 34.5 = 110.5 \text{ cm}$	
	Eccentric spun package, at full spun package size	$\lambda_5 = d_W \cdot \pi = 40 \cdot 3.14 = 125.6 \text{ cm}$	
	Same fault, measured on drawn yarn (cops)	$\lambda_6 = R_V \cdot \lambda_5 = 3.2 \cdot 125.6 = 402 \text{ cm}$	
	Traverse, measured on spun yarn	$\lambda_7 = \dfrac{v_P}{H_D} = \dfrac{900}{340} = 2.65 \text{ m}$	
	Traverse, measured on drawn yarn (cops)	$\lambda_8 = R_V \cdot \lambda_7 = 3.2 \cdot 2.65 = 8.48 \text{ m}$	
	Godet (roll) eccentricity, measured on spun yarn	$\lambda_9 = d_G \cdot \pi = 12 \cdot 3.14 = 37.7 \text{ cm}$	

	Cause	Calculation of wavelength range		Fault category
Spinning machine	Gearbox of the drive roll	normally shorter than $\lambda_7{}^*$		1/3/4/5
	Gearbox of the spun package drive shaft	normally shorter than $\lambda_7{}^*$		1/3/4/5
	Turbulence beneath spinneret	normally between 1...100 m		almost periodic
	Turbulence caused by quench air	normally between 1...100 m		almost periodic
	Extruder	normally greater than 1000 m**		1/3***
drawtwister	Godet (draw roll) eccentricity, upper roll	$\lambda_1 = d_G \cdot \pi \cdot R_V = 12 \cdot 3.14 \cdot 3.2 = 120.6 \text{ cm}$		1
	Godet (draw roll) eccentricity, lower roll	$\lambda_2 = d_G \cdot \pi = 12 \cdot 3.14 = 37.7 \text{ cm}$		1
	Spindle eccentricity: empty tubes	$\lambda_3 = d_H \cdot \pi = 4.5 \cdot 3.14 = 14.1 \text{ cm}$		1
	Spindle eccentricity: full packages	$\lambda_4 = d_S \cdot \pi = 10 \cdot 3.14 = 31.4 \text{ cm}$		1
	Traveler defective	$\lambda_5 = d_R \cdot \pi = 15 \cdot 3.14 = 47.1 \text{ cm}$		1/3/5
	Ring rail period: empty tubes	$\lambda_6 = t_1 \cdot v_P = 7 \cdot 36 = 252 \text{ m}$		3
	Ring rail period: full packages	$\lambda_7 = t_2 \cdot v_P = 5 \cdot 36 = 180 \text{ m}$		3

(continued)

Figure 7.33 (*continued*)

Causes of perodic and nearly-periodic defects at high speed spinning

Material	Polyester	Max. package diameter $d_S = 30$ cm
Final titer	T_E = dtex 50f20	Spinning pump throughput per rev.
		$V = 5$ cm^3

Production speed $V_P = 4500$ m/min   Density $\rho = 1.346$ g/cm^3
Spinning tube outside diameter $d_A = 11$ cm
Package stroke $b_S = 20$ cm   Traverse double strokes $H_{D'} = 1450$ min^{-1}
Required draw ratio at drawtexturing (see fig. above) $R_v = 1.4$
Titer of (high speed) spun yarn $T = R_v \cdot T_E = 1.4 \cdot 50 = 70$ dtex $= 7$ Tex
Required polymer throughput per minute $F_{tot} = t \cdot V_P \cdot 10^{-3} = 7 \cdot 4500 \cdot 10^{-3} = 31.5$ g
Spinning pump throughput per rev. $F_P = \rho \cdot V = 1.346 \cdot 5 = 6.73$ G

	Cause	Calculation of wavelength range		Fault category
	Spinning pump period	$\lambda_1 = \dfrac{v_P \cdot F_P}{F_{tot}} = \dfrac{4500 \cdot 6,73}{31.5} = 961$ m		1/3
	Eccentric spun package: almost no yarn	$\lambda_2 = d_A \cdot \pi = 11 \cdot 3.14 = 34.5$ cm		1
	Eccentric spun package: full package	$\lambda_3 = d_S \cdot \pi = 30 \cdot 3.14 = 94.2$ cm		1
	Traverse	$\lambda_4 = \dfrac{v_A}{H_D} = \dfrac{4500}{1450} = 3.10$ m		2/3/4
	Drive roll transmission	normally shorter than λ_4 *		1/3/4/5
	Spun package drive shaft	normally shorter than λ_4 *		1/3/4/5
	Turbulence beneath spinneret	normally between 1...100m		almost perodic
	Turbulence due to quench	normally between 1...100m		almost perodic
	Extruder	normally greater than 1000m ***		1/3***

HIGH SPEED SPINNING MACHINE

* The gearing is required for exact calculation
** Can be deduced from diagram by repetitive measurement within a package
*** Almost perodic defects can also occur here, depending on the cause

Table 7.11 Example of an Investigation into the Factors Affecting the Uster Value [81]

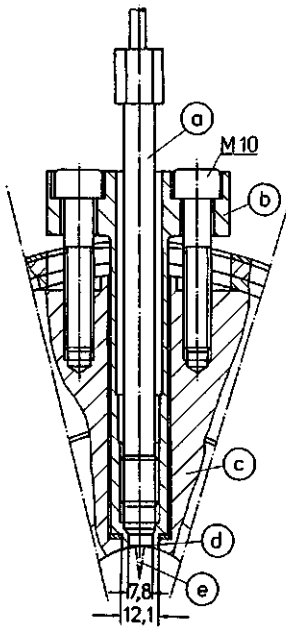| Description	Variable	Affects	Periodicity	Example from investigation c_1-determined approx. component	CV component %
e_1	Molecular weight uniformity	Viscosity	None	0.08	0.6
e_2		Melt tensile strength	None	0.1	0.5
e_3	Melt temperature (beneath spinneret)	Viscosity	Depends on temperature fluctuations	0.14	0.85
e_4		Melt tensile strength			
e_5	Melt pressure variations, pressure variations due to spin pump	Throughput	Pump speed	0.06	0.4
e_6	Quench air and turbulence	Cooling	Irregular	0.21	0.8
e_7	Filament position in bundle	Cooling	None	0.06	0.2
e_8	Yarn tension				
e_9	Traverse		Stroke frequency	0.2	0.43
e_d	Diverse, unknown sources			0.15	0.5
				1.00	$CV = 0.613$

Figure 7.34
Example of installation of a Dynisco melt pressure—or melt temperature sensor (a) with intermediate flange (b) in a machine wall (c), with flat membrane (d) for pressure—or with sword (e) for temperature measurement [30]

7.9   Temperature Measurements, Melt Pressure Measurements

These measurements require a high degree of precision, and if the sensor is located in the melt or solution, particular care must be taken that there are no dead spots formed at or around the probe where stagnant polymer could form. The insertion must be correct in terms of polymer flow and must be robust enough so that it does not break off at, e.g., low melt temperature. Installations such as a sword-shaped probe dipping into the fluid or a tangential membrane are preferred. In order to enhance the machine appearance, the probe is often provided with a flange fitting (Fig. 7.34).

7.9.1   Temperature Measurement

The type of temperature-measuring element required can be selected for the required temperature range from Fig. 7.35. In Europe, resistance thermometers—particularly Pt100—are preferred for use up to 500 °C. After calibration, these are more exact than the thermocouples preferred in the USA, which, however, have the advantage of small size, being almost point-sized. The smallest Pt100, diameter = ca. 3 mm × length = ca. 8 mm, is usually adequate.

Standard elements according to DIN or ASME, although slightly different, are obviously acceptable. Semiconductors (thermistors) have a large temperature gradient and furthermore their response changes so rapidly that they need to be recalibrated within a year. Above 450 to ca. 1000 °C, NiCr-Ni thermocouples can be used, and above this—up to ca. 1300–1400 °C—PtRh-Pt thermocouples. As thermocouples indicate the temperature difference relative to a cold junction, the constancy of the latter must be maintained. For measurement of still higher temperatures, radiation pyrometers are used.

For measurement of external surface temperatures, use is made of contact (or so-called secondary) thermometers. One can also use temperature-sensitive colored pencils or temperature dye characteristic bodies. Here attention must be paid to the time specified for the color change.
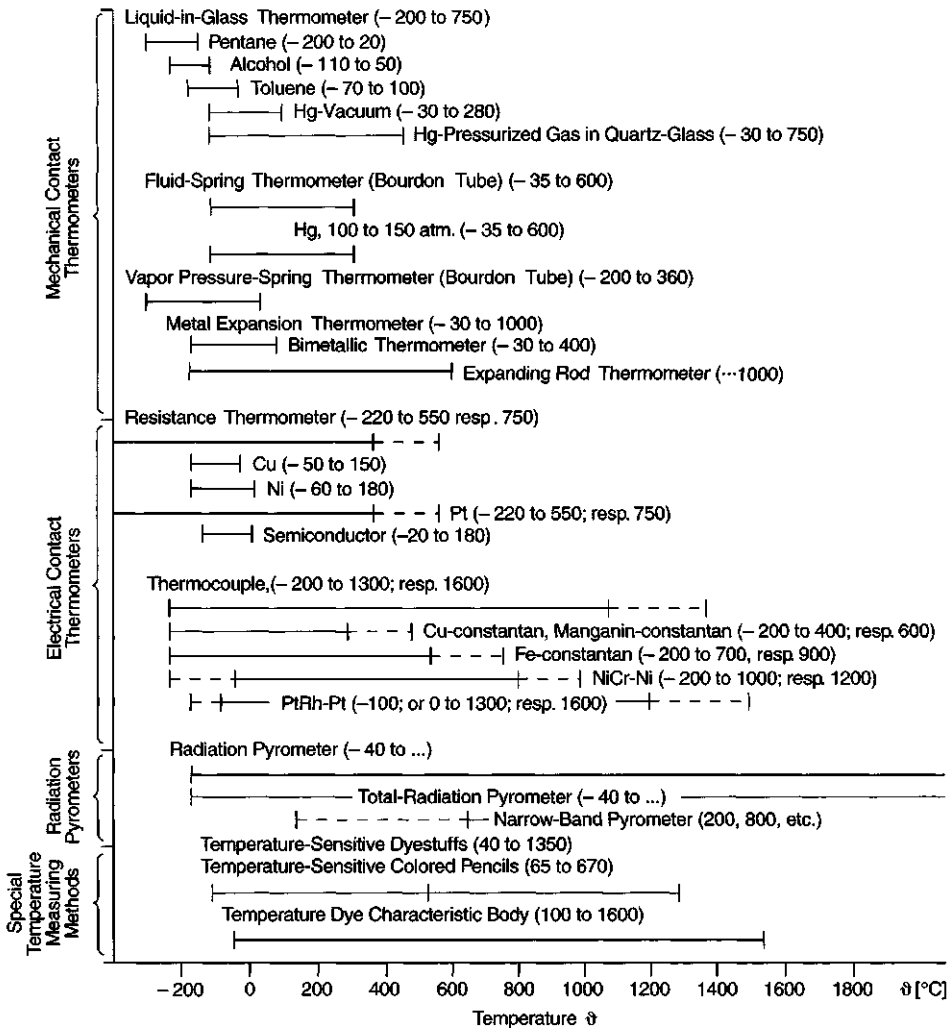
Figure 7.35 Application ranges of temperature measuring elements or apparatus
———— usual, — — — — — seldom-used range

Pt100 resistance thermometers should preferably be used in a 3-wire configuration to take into account the distance between the sensor and the indication or controller. As the effect of temperature and resistance on the leads of a 4-wire configuration are insignificant, these are even more preferable.

A selection of temperature sensor mountings is shown in Fig. 7.36:

a) for chemical apparatus, with standard connection head
b) as per a), but for measurement in air or gas
c) for spinning beams, spin extruders, inter alia, the preferred form, often with a contact cone on the front surface and an extension piece between the measuring point and the surface of the insulation, if fitted.
d) two special elements for use in confined spaces, e.g., for temperature measurement immediately below a draw roll surface (Fig. 4.200 B)
e) for measurement of surface temperature
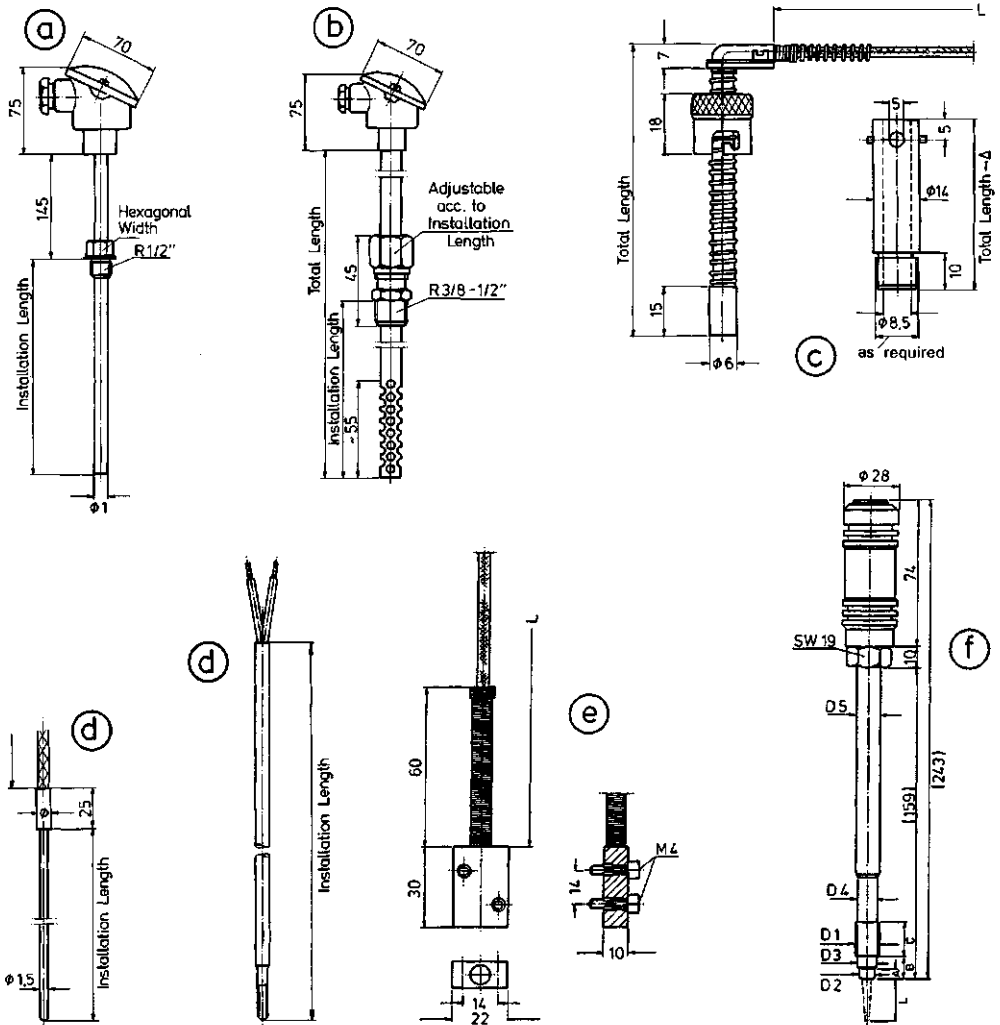
Figure 7.36 Installation configuration of commercially-available temperature sensors (for explanations of a) to f), see text)

f) for melt temperature measurement using an immersed sword probe of length L (at least 15, preferably up to 40 mm). (This can be incorporated into the Dynisco pressure sensor, Fig. 7.38.)

These constructions are valid for both resistance thermometers and thermocouples.

The measuring element should be inserted against the polymer flow, or—in the case of condensation heating—in the vapor space. For low viscosity fluids and vapors, the elements are placed in a welded pocket for ease of removal, while for measurements in metal bodies, the element is placed directly in a hole bored into the body. For good thermal contact with the measuring surface, a 120° cone is better than a flat base at the bottom of the tube. In solutions and melts, the elements are inserted directly into the fluid, using, e.g., bolts and flanges (e.g., as per Fig. 7.34). In measurements in fluids or vapor, the further the measuring element is from the tube wall, the more exact is the measurement. When built into heated metal bodies, the measuring sensor should not be more than 20 (to 25) mm away from the source of heat in order to avoid too great a temperature hysteresis in the body.
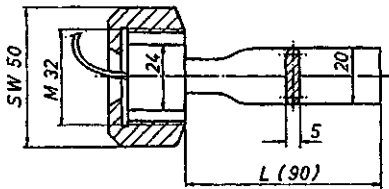
Figure 7.37
Tongue gauge pressure sensor for pressure ranges of 0 ... 30 to
0 ... 300 bar [62]
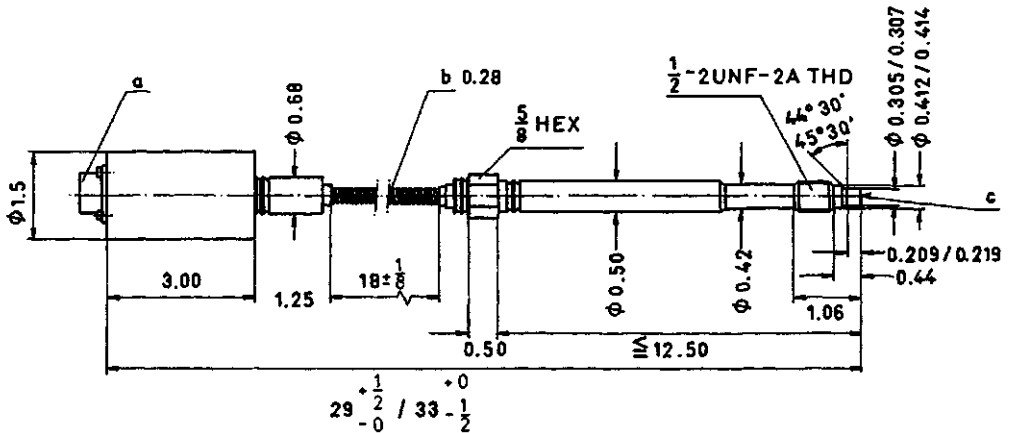
Figure 7.38   Dynisco melt pressure measuring element [63], measuring range 0 ... 250 to ... 2000 bar at
temperatures up to 400, respectively 700 °C. (Dimensions in inches). Smallest measuring range
0 ... 10 bar (opto-electronic).

For display and recording—unless it is integrated in the microprocessor—thyristorized instruments are used which have digital display increments of 1, 0.5 or 0.1 °C. Too fine a digital display increment can lead to flutter after the decimal point and give the false impression of higher accuracy. In many control circuits, ± 0.5 °C is called for; this is synonymous with an accuracy of ± 0.2 °C in the individual components (installation, measuring element, display, etc), and, at 300 °C, demands an instrument of the 0.05% class.

Often a single display is used to serve many measuring elements, a press button being used to call up the required temperature: this is acceptable for readings which are seldom required or for automatic scanners. Separately wired, double measuring elements, each having its own display, are recommended for important positions, for measuring and controlling and for recording or printing.

7.9.2   Melt and Solution Pressure Measurement

Since melts, and possibly solutions, block dead spots and can depolymerize or crack there, sensors which protrude into the fluid must be tangential to the fluid and not result in the formation of dead spots. The required sensors are either of the tongue type or are pressure membrane sensors having either a transmitter fluid or an electrical measuring bridge and corresponding display equipment.

Tongue pressure sensors (Fig. 7.37, for example [62]), like membrane pressure sensors of this type, usually have a mercury filling, the displacement of which is measured by a flat- or spiral spring manometer (Bourdon gage). The output signal is transmitted via a rotary potentiometer. Because of the mercury filling, these sensors are temperature sensitive, and must therefore be calibrated at their operating temperature. Membrane sensors are available in the ranges 0 ... 6 bar and up to 100 bar, while tongue sensors cover the range 0 ... 30 bar up to ca. 400 bar.

Electrical pressure sensors—e.g., "Dynisco" [63]—have a sensing membrane of only 7.75 mm diameter and incorporate an internal resistance-measuring bridge. They are available in discrete pressure ranges, from 0 … 10 bar up to a few thousand bar, and for temperatures up to 700 °C. One should nevertheless select a sensor which closely matches the actual operating pressure and temperature ranges.

Figure 7.38 shows such a "Dynisco" sensor, complete with connecting head. The machine installation can also be enhanced by fitting an intermediate flange, as in Fig. 7.34.

When a product (large area) filter is fitted between the spin extruder and the spinning pumps, the controlling pressure sensor should be located before the spinning pump, and an additional alarm pressure sensor before the filter to monitor the effective extruder pressure.

The pressure controller and display must have:

- a low pressure contact alarm. This alarm is bridged for start-up, but activates, when the pressure subsequently drops below a minimum, in order to switch off the extruder for reasons of low melt flow, awaiting polymer charging.
- a control range which can be set, comprising maximum/minimum switching.
- a high pressure contact alarm, in case the extruder pressure unexpectedly rises too high.

Typical pressure application ranges are:

For	Viscosity, P	Pressure range, bar	Precision: the lower of	Measurement sensor
Solutions	100 … 400	3 … 6 … (10 … 30)	< ± 10%, < ± 1 bar	Tongue sensor
Melts	600 … 1200	40 … 120	< ± 3 bar, < ± 3%	Membrane sensor
	1200 … 2500	60 … 150	< ± 3 bar; < ± 3%	Membrane sensor
	2500 … 5000	60 … 200	< ± 3 bar; < ± 3%	Membrane sensor
	… 20000	… 700	< ± 3%	Membrane sensor

7.9.3   Moisture Measurement

Moisture is liquid taken up on or in the material and is defined in DIN [89]. Water of crystallization is excluded from this definition. The moisture content (on a dry basis) is given by $(m_m - m_d)/m_d$, where the indices $m =$ moist and $d =$ dry, and m refers to the mass [90].

For normal textile moisture contents 1 … 17%, it is usually sufficient to weigh the material in the moist and dried states. In the case of conditioned samples, the sample is considered conditioned if its weight does not change by more than 0.05% over a 10 minute period (according to DIN).

For the quick checking of the moisture content of staple bales, it is often sufficient to insert a hygrometer [92]. This works by an absorption principle and is not very accurate. Measurement using the Turbo tester gives relatively accurate results, but is seldom used [91]. Here a defined quantity of air $(m_{yarn} \gg m_{air})$ is forced through a fiber sample in a closed air loop. The electro-capacitive, electrostatic and thermo-electric measurement processes are no longer used because of the cost of the apparatus and the availability of modern chemical methods.

In the distillation process, the yarn sample is added to a high boiling point liquid (toluene, xylene, etc.) in a glass flask and heated. The water in the distillate is measured volumetrically. The method is very accurate, and the test requires only 15 … 30 min. In the extraction process, water is removed by n-H_2SO_4 (e.g.), and the extract is then titrated with Iodine.

All the above processes have been superseded by simple, automatic moisture measuring equipment which can give greater accuracy in a shorter time: the Karl Fischer method (similar in principle to the extraction process), the DuPont Moisture Tester and the Aquatrac Moisture Meter [92].

In the Aquatrac system, the water reacts with calcium hydride to give hydrogen gas:

$$CaH_2 + H_2O \longrightarrow Ca(OH)_2 + 2H_2$$
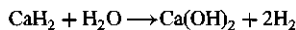
in an electrically heated reaction vessel. The hydrogen evolved causes the pressure to rise. The pressure, directly proportional to the water content, is measured by a piezoresistive pressure transducer. The sample is first weighed, the weight is given to the Aquatrac and the sample is placed in the test chamber, which is

evacuated to a pressure of 5 mbar. The sample is then heated to one of five temperatures between 80 and 190 °C. The pressure transducer automatically calculates the % moisture content. Depending on the sample holder size and the fiber (bulk) density, sample weights of between 0.5 and 96 g are possible. The normal measurement range is from 0 to 0.1...4%. The measurement deviation is ±2% of the measured value ±1% of the measurement range. A specially modified version (for PET, amongst others) can accurately measure moisture contents below 10 ppm H_2O.

In the Karl Fischer method, the water is removed by heating the sample in an oxygen-free, dry nitrogen stream at about 200 °C, is absorbed in anhydrous methanol and subsequently titrated with Karl Fischer reagent (KFR). The activity factor T of KFR (mg H_2O per ml KFR) is first determined by titration. About 15 g (E) of material to be tested is heated and the water envolved is absorbed in 50 ml of methanol, which is then titrated with KFR, requiring A ml. The moisture content of the sample (%) is then given by [93] $A \cdot T/(10 \cdot E)$.

7.10   Fluid Mechanics

Although aero- and hydrodynamics are among the best-researched areas in physics, both mathematically and experimentally [48, 49], flow processes for Re < 100 and particularly for <0.1 have not been thoroughly researched, and there is little published in this area. These regions are, however, the important ones for polymer flow. Table 7.12 gives guide values for some polymer melts and solutions, which—due to polymer properties—can vary widely in comparison with water and air. At typical flow velocities (Fig. 4.118) in a 20 mm pipe, the Reynolds numbers of melts range between 0.003 and 0.05. The Reynolds number for air flow in quench chambers is about 0.3...50, while that for melts flowing through filters can be as low as 10^{-6}.

Table 7.12a   Flow Properties of Fluids

Substance	Temperature °C	Spec. weight kg/m³	Density kg s²/m⁴ $\approx \gamma/g$	Viscosity $\eta \cdot 10^6$ kg·s/m²	Kinematic viscosity $v \cdot 10^6$ m²/s
Water	20	998	101.7	102	1.01
	60	983	100.2	47.9	0.478
	100	958	97.85	28.8	0.295
Air	20	1.20	0.123	1.85	15.1
	100	0.95	0.096	2.22	23.1
	200	0.746	0.076	2.66	35.0
Caprolactam	80	1013.5	103.3		
DMT	180	1080	110.1	see pages	
Ethyleneglycol	20	1113.6	113.5	831–832	
	180				
PA 6	270	970	98.9	$14.8 \cdot 10^6$	$0.15 \cdot 10^6$
PA 66	285	980	99.9	$8.6 \cdot 10^6$	$0.86 \cdot 10^5$
PET	290	1250	127.4	$28.4 \cdot 10^6$	$0.22 \cdot 10^6$
PP	250	780	79.5	$40.7 \cdot 10^6$	$0.5 \cdot 10^6$
PAN (25% in solution)	100	1000	102	$2.5 \cdot 10^6$	$2.45 \cdot 10^4$
PE (7% in decalin)	180	960	97.9	$1.2 \cdot 10^9$	$12.3 \cdot 10^6$

Table 7.12b Density and Viscosity of Various Substances

Substance	Temperature	Spec. weight	Density	Viscosity η			Kinematic viscosity
	°C	$\gamma(\text{g/cm}^3)$	$\dfrac{\gamma}{g}\left(\dfrac{\text{kg s}^2}{\text{m}^4}\right)$	(P)	(Pa·s)	kg s/m^2	m^2/s
PET (0.95 IV)	310	1.22	124.4	10^4	10^3	10^2	0.82
PP	260	0.7	71.36	5000	500	51	0.715
PET (0.63 IV)	285	1.25	127.4	2500	250	25.3	0.20
PA 6	265	1.00	102	1000	100	10.2	0.1
PA 66	285	1.00	102	750	75	7.65	0.075
				100	10	1.02	
Solution	150	1.00	102	200	20	2.04	0.02
Water	90	0.985	32.6	$3.2 \cdot 10^{-3}$	$3.2 \cdot 10^{-4}$	$3.26 \cdot 10^{-5}$	$0.3 \cdot 10^{-6}$
	20	1.00	102	10^{-2}	10^{-3}	$1.02 \cdot 10^{-4}$	10^{-6}
Air	200	$0.75 \cdot 10^{-3}$	0.076	$2.61 \cdot 10^{-3}$	$2.61 \cdot 10^{-5}$	$2.66 \cdot 10^{-6}$	$3.5 \cdot 10^{-5}$
	20	$1.2 \cdot 10^{-3}$	$1.22 \cdot 10^{-1}$	$1.81 \cdot 10^{-3}$	$1.81 \cdot 10^{-5}$	$1.85 \cdot 10^{-6}$	$1.51 \cdot 10^{-5}$

7.10.1   Air Flows for Re $= 0.1 \ldots 500$

For flow through pipes and along plates, the transition from laminar to turbulent flow is generally characterized by $\text{Re}_{\text{crit}} \approx 2300$ and a cone angle of 7°. In contrast, for the above-mentioned flow range [65],

$\text{Re}_{\text{crit}} \leq 80$ and the cone angle $\approx 12°$;

this is demonstrated, inter alia, in Fig. 7.39 [65] and is valid for flow through

- fine-woven wire mesh, when Re is based on the maximum velocity through the mesh [66] and $\text{Re}_\beta = \text{Re}/\beta$, where $\beta = 1 - (d/T)^2$, $d =$ wire diameter and $T =$ pitch. From the above, the resistance coefficient $\xi = \Delta p / \dfrac{\rho}{\delta} \dfrac{v^2}{v}$ in Fig. 7.40 can be calculated [66].
- Dutch weave (in which the fine wires running in one direction lie close to one another, having $T = d$). This has approximately the same resistance curve as Fig. 7.40 when one substitutes $\text{Re}_{1\mu} = \text{Re}_\beta/100$. One is here only considering those Dutch weaves where the air exits the screen normally, not at an angle (Fig. 7.40a, b).
- perforated plates, as defined in Fig. 7.41. These always have turbulent exit flow. The resistance coefficient ξ depends only on the free area ratio β (Fig. 7.41).
- sintered metal surfaces. The air flow rate through these surfaces depends on the pore fineness and the pressure difference, as shown in Fig. 7.42. When used for radial quenches, the required inlet pressure is $100 \ldots 600$ mm WG for a velocity range of ca. $0.1 \ldots 1$ m/s. The bend in the curve at ca. 0.1 m/s (Fig. 7.43) shows that the flow becomes turbent above 0.1 m/s; this is confirmed by the turbulence measurement in Fig. 7.44, which shows a ca. $\pm 10\%$ variation relative to the mean velocity with time and a ca. $\pm 50\%$ variation with distance. This arises from the statistical variation of particle size, pore size and their distribution.
    Figure 7.45 gives the air velocity profile along a quench candle 1.2 m high × 0.1 m diameter. Because of the high ξ value, the velocity becomes constant beyond 0.3 m from the air entry. In contrast to this, a similar quench candle made out of fine wire mesh has an air velocity profile that is 10 times higher immediately below the top end than 0.2 m lower down. Below this, the velocity decreases rapidly to ca. $0.03 \ldots 0$ m/s.
- a bend in the flow direction of angle δ also results in a resistance coefficient (see Fig. 7.46).
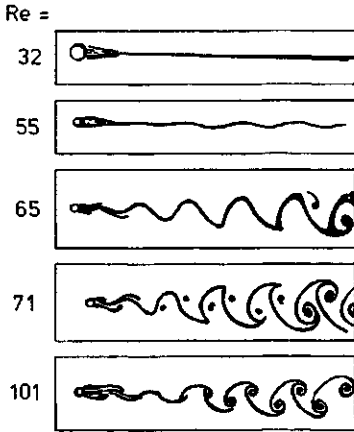- resistance coefficients of various solid and permeable bodies are given in Table 7.13a for Re < 200.

Re =

Figure 7.39
Streamlines behind a small cylinder according to Homann [65]
(photograph from [70] shown, $Re_{crit} \approx 60$).

a)

b)

c)

Figure 7.40a
Fine-wire woven mesh:
photographs of examples
[67].
a) Twill weave
b) Reverse plain Dutch
  weave: air flow normal
  to screen
c) Dutch twilled weave:
  air flow at an angle to
  screen—unusable

Figure 7.40
Resistance coefficient of fine-wire woven mesh; $Re_\beta = Re/\beta$;
$\beta = 1 - (d/T)^2 = $ free area ratio
A: $\zeta = 0.72 + 49/Re_\beta$; W: measurements according to Wieghardt

7.10.2   Laminar and Turbulent Flow

A characteristic of turbulent flow is that the three velocity components in $(u^2 + v^2 + w^2)/\bar{V}^2 = Tu$ exceed a given value, e.g., 0.01 or 0.015. This is certainly the case for air ducts; on account of their dimensions and $\bar{V} \approx 8 \ldots 2$ m/s, $Re_{crit} \geq 2300$. The degree of turbulence almost always lies between 0.15 and 0.3, and continues up to the quench chamber air rectifier.

The air rectifier must reduce the degree of turbulence down to ≤ 0.01. Fine wire woven mesh serves to damp turbulence [68], each layer reducing the turbulence by $\sqrt{1 + \xi_n}$. The damping decrement of a set of n meshes having a mesh distance $\gg$ mesh aperture is given by $D = \prod_{n=m} \sqrt{1 + \xi_n}$ Fm/Fn [69]. According to the sample calculation in Table 7.14 (p. 688), the degree of turbulence is reduced from ca. 0.3 to 0.011 by the third sieve and from 0.011 to 0.0015 on exiting the fourth sieve. Both these latter values are adequate for laminar quench cabinet cooling.
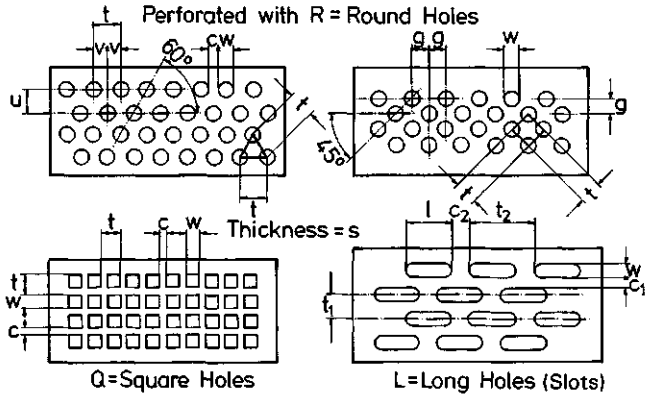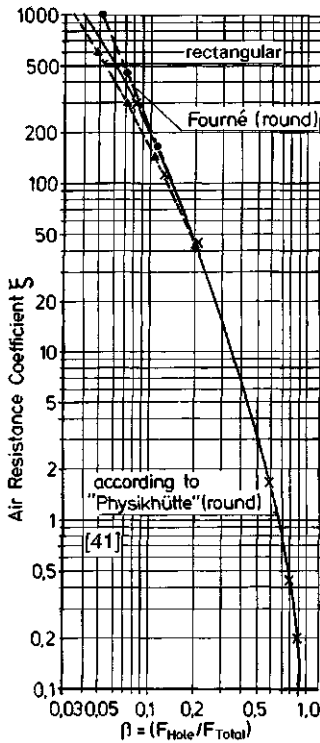
Figure 7.41 Resistance coefficients of perforated plates during air flow, as a function of the free area ratio and hole definition

R circular-edged holes, 60° displaced

R circular-edged holes, 90° displaced

Q Square-edged holes

L Slotted holes

$\beta = k\,(w/t)^r$: for $R60°$ $R45°$ $\square Q$

$$\beta = 0.907 \quad 0.785 \quad 1$$

$\beta = (w/t_1 t_2)(1 - 0.25\,w^2)$ for L
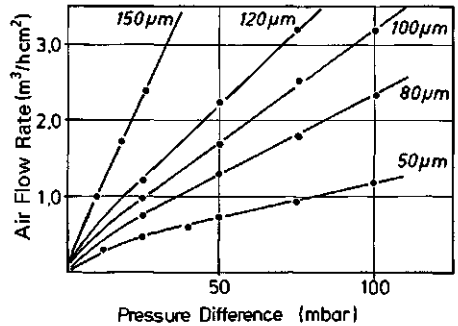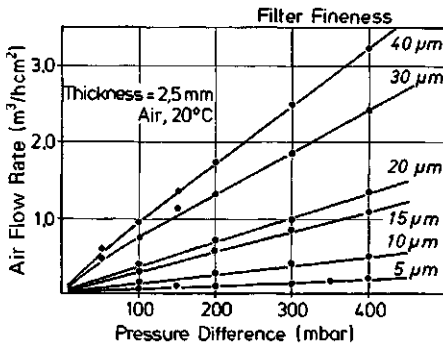
Figure 7.42 Air permeability of sintered metal surfaces [87]

The above does not apply if the sieve distance is too small [71]. Two or more similar sieves superimposed give rise to a Moiré pattern, i.e., the air flow resistance becomes periodically less—and more dense along the length of the sieve set. The air flow rate in the densest areas is reduced in the same way as when the screen blocks up with dirt (section 4.7.4.1). There is a shear gradient in the transition zone which causes turbulence.

Laminar air flowing into a cooling chamber is subject to the flow laws of a large, rectangular air duct, i.e., a new boundary layer having a thickness $\delta = 3\sqrt{L/\bar{V}}$ forms on the walls [70]. This flow also undergoes a transition to turbulence as soon as $\mathrm{Re} = \bar{V}\cdot L/\gamma \geq 2300$ (see section 3.3.2).
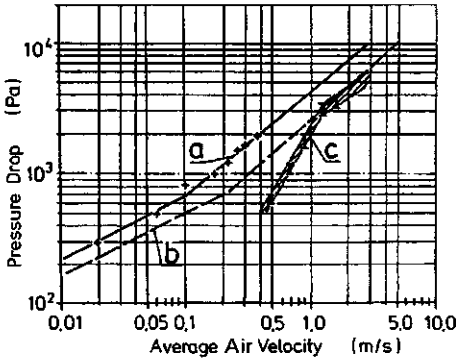
Figure 7.43
Pressure drop through a sintered metal quench candle [87]
a) at ca. 30 mm distance from the surface
b) at the surface: see Fig. 7.42
c) additional measured values to (*b*): fineness 100 μm, s = 3 mm (measured by Fourné)
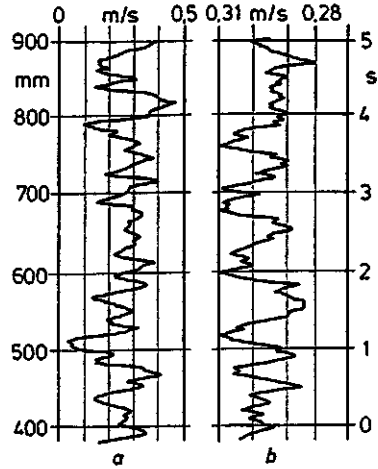
Figure 7.44
Turbulence measurements on a sintered metal candle according to Fig. 7.43 and 7.45
a) along the candle length [mm] and b) with a stationary measuring element to give a time-dependent result (Fourné)
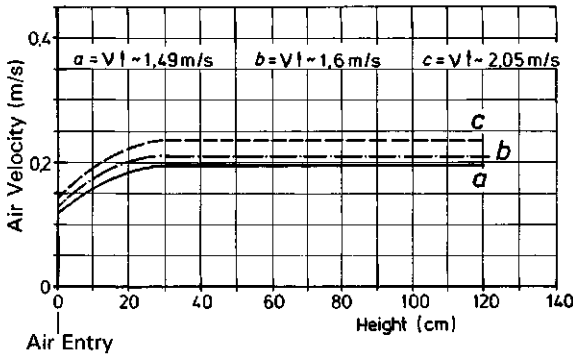
Figure 7.45   Air velocity profile of a quench candle of 0.1 m diameter × 1.2 m height [87]
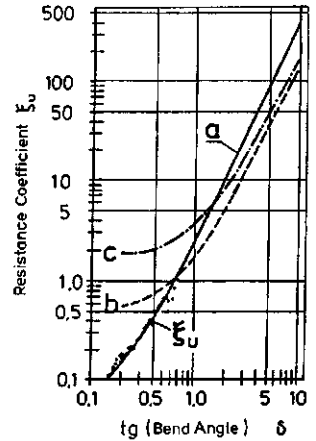
Figure 7.46
Resistance coefficient of a bend of air stream angle δ

The velocity profile in a tube or between two walls also depends on the type of flow: there is always adhesion to the walls. The velocity distribution is parabolic (2nd power) in laminar flow and is described by a 7th power law in turbulent flow; this arises from the intensive energy exchange, which also occurs perpendicularly to the direction of flow. At higher viscosity the curve approaches an nth power polygon fit; at 5000 P, e.g., a 4th power fit applies (Fig. 4.87). Extremely slow, so-called creep flow, corresponds

Table 7.13   Various Flows and their Corresponding Approximate Reynolds Numbers

Medium, state	Velocity m/s	Flow regime	Definition	Dimensions	Re
Water 20°C	2	Pipe		$\varnothing$ 10 mm	20 000
				$\varnothing$ 100 mm	200 000
Air 20°C	6	Square duct	1 m²	$\square$ 1.13 m	448 000
			0.5 m²	$\square$ 0.8 m	317 000
	3	Duct acc. to BS		20 × 617 mm	41 265
	1	Air rectifier mesh	3700 M/cm²,	0.063 mm $\varnothing$, $\beta=0.38$	11
			1000 M/cm²,	0.125 mm $\varnothing$, $\beta=0.36$	23.6
			580 M/cm²	0.16 mm $\varnothing$, $\beta=0.38$	27.9
	0.5	Quench air cooling chamber with inlet damping ~0.5 mm	$L \cdot Re_K = 4200$	$Re = 0.2$ m$:L_{Tu} = 0.63$ m $B_i = 0.67$ m$:L_{Tu} = 0.19$ m	$Re_B = 6620$ = 21 630
Solution 70...150°C	0.1	Manifold pipe	125 l/h $\triangleq$ 30 kg/h $\gamma=0.02$ m²/s	$\varnothing$ 15	$Re = 0.075$
	0.4331	Spinneret hole (bore)	0.1 g/min = 5 dtex	$\varnothing$ 70 µm; 50 m/min; $c=0.25$	0.0015
Polymer melt	0.05	Main PA 6	100 kg/h $\gamma=0.1$ m²/s 10 000 kg/h	$\varnothing$ 26.6 mm	0.0133
	0.071	PET	$\gamma=0.2$ m²/s	$\varnothing$ 200 mm	0.071
	0.000271	Spin pack block	167 dtex PET 3600 m/min $\triangleq$ 78.16 g/min	spinneret $\varnothing_{OD}$ 80/$\varnothing_{ID}$ 70	$9.5 \cdot 10^{-5}$
	0.638	Spinneret capillary (as before, 62f)	0.2 mm $\varnothing$	52 holes, otherwise as before	$6.38 \cdot 10^{-4}$

Table 7.13a   Resistance Coefficients ξ for $Re \leq 200$

	$\zeta =$
Disk (90° to flow direction)	$64\pi/Re$
Sphere, ball	$24/Re$
Cylinder (axis 90° to flow direction)	$8\pi/Re$ (2-ln Re)
Woven mesh	$0.72 + 49/Re_\beta$
Sand	$94/Re^{0.16}$ to $2000/Re$
Pipe	$0.3164/Re^{0.25}$
Gap, slot	$0.1187/Re^{0.25}$
Flow along wall (single-sided)	$1.327/\sqrt{Re}$

on the other hand to a potential flow [70]. From this it follows, e.g., that slow melt flows having Re < 0.01 develop streamlines which are extremely stable.

7.10.3   Heat Transfer from Yarn to Air

In the case of filaments extruded from the spinneret and taken up at high speed, it is to be expected that, given the short transit time, the individual filaments can only transfer their heat to the axially-developed boundary air layer, i.e.—excluding radiation—the filament gives up only that amount of heat which the boundary layer can transport away. This boundary layer is then transported away by the cross-flow

Table 7.14 Turbulence Damping by Means of Woven Mesh Screens (Screen Separation $\gg T$)

Mesh number $1/cm^2$	Free area β	Wire diam. mm	Re_β for $v = 0.5\,m/s$	ζ	$\sum_n \zeta_n$	$\prod_n \sqrt{1 + \zeta_n} = D$	$Tu[\%]$ for $Tu_0 = 0$
700	0.38	0.14	12.2	4.74		2.396	
					4.74		0.083
1500	0.38	0.1	11	5.17		5.951	
					9.91		0.034
2500	0.37	0.08	7.16	7.56		17.41	
					17.47		0.011
3700	0.38	0.063	5.49	9.65		56.82	
					27.12		0.0015
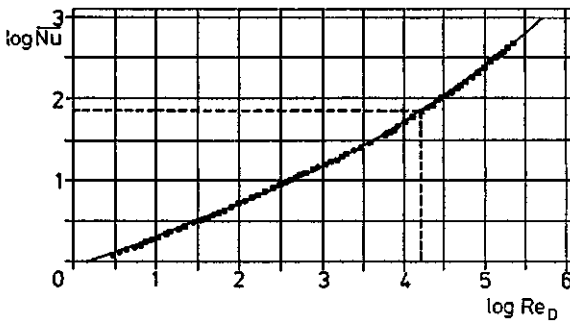
Figure 7.47
Nusselt number as a function of the Reynolds number

quench. From this it follows that increasing the take-up speed, in contrast to the quench velocity, results in only an inconsequential increase in the heat transfer. On this basis, the surface heat transfer coefficient α can be calculated from the Nusselt number, which itself—according to Fig. 7.47—is a function of the Reynolds number of the cross-flow quenched yarn cylinder ($\alpha = Nu \cdot \lambda/D$, $\lambda = $ thermal conductivity of air $= 0.0150\,k\,cal/m\,h\,K$ at $20\,°C$ and 0.0208 at $100\,°C$ and 1 bar).

7.11   Construction Materials

For all parts which do not come into contact with pre-, intermediate or final products, the normal materials of construction of machines and apparatus are used.

For parts coming into any kind of contact with production materials, the following recommendations are made:

1. Welded parts coming into contact with monomers, additives, melts, solutions, etc.
   - for higher corrosion resistance, except for PET and its pre-products
   - for chlorine-containing cooling water

material 1.4541 (up 550 °C) or 304 L
1.4571 (up to 400 °C) or 316 L
1.4462 (>20% Cr, <10% Ni) (only in emergencies, 1.4571 up to ca. 80 ppm Cl, <100 °C, short term)

2. Turned parts (without welding)   1.4305
3. High tenacity parts up to 400 °C   1.4122
   (for example, small extruder screws)
4. Parts running against items 1 . . . 4,   1.4006
   Extruder cylinders, internally centrifuged with   Xalloy 306 or Reiloy R121
5. Moving parts, from standard steels   Ck 45—Ck 60—St 50—St 60—
                                                                     50 Cr V4 (42 Cr Mo 4)
6. Spinnerets (up to 400 °C)   1.4580 or 1.4571 (better 1.4549
                                                                     or 1.4057)
7. Dowtherm-heated boxes, autoclaves,   boiler plate steel HII
   heating jackets, welded-in tubes for calrod heaters, etc.   (= 1.0425)
8. Machine and welded parts up to
   600 °C   1.4948 = X6 Cr Ni 18 11
   750 °C   1.4909 = X2 Cr Ni Mo N 17 12 [72]
9. Electric resistance heater plates
   up to 350 °C   electric resistance wire encased
                                                                     in mica sheet or "Mekanit", or
                                                                     electric calrod heaters cast in AlSi
                                                                     (without Mg!)
   up to 550 °C   electric calrod heaters cast in Ms
   up to 650 °C   stainless steel calrod heaters cast
                                                                     in Gg 40

10. Screws for normal loads and ≤350 °C
                                                                     10.9 (hot-rolled screws)
                                                                     12.9 for low elongation
    for 200 . . . 500 °C
    nuts   24 Cr Mo 5
    screws, bolts   21 Cr Mo V511 (preferred)
                                                                     (possibly 24 Cr Mo V55)
    stainless steel   1.4541

For dimensioning, the $\sigma_{0.2}$ limit is recommended; for torsional strength, one can estimate using $0.8 \cdot \sigma_{0.2}$ if no better figures exist (Fig. 7.48)
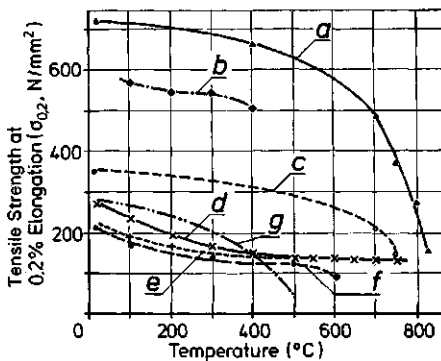

Figure 7.48
$\sigma_{0.2}$ tensile strength of various construction materials as a function of temperature
a) Inconel 700
b) X15 Cr Mo 17
c) Hastelloy C
d) X2 Cr Ni Mo N 1712
e) X10 Cr Ni Mo Ti 1810
f) X10 Cr Ni Ti 18.9
g) C (k) 35 St 35.8

Comparison of Steels

German material number	DIN (EN)	AISI (USA)	BS (GB)	Main usage
1.0037	St 37-2 (S235JR)	1015	FE 360 B	Construction steel,
1.0060	St 60-2 (E335)	A572 Gr.65	FE 590-2FN	welded parts
1.0425	H II (P265GH)	–	1501	Boiler plates, dow boxes
1.7035	10.9 = 41 Cr 4	5140	530	Warm rolled screws
1.7225	12.9 = 42 Cr Mo 4	4140	708	Low elongation screws
1.8070	21 Cr Mo v. 5–11	–	–	Screws
1.7258	24 Cr Mo 5	4130	708A25	Nuts ≤ 500 °C
1.4948	X6 Cr Ni 1811	–	–	≤ 600 °C) Construction
1.4909	X2 Cr Ni Mo N 1712		–	≤ 700 °C) and/or welded parts
1.4006	X10 Cr 13		410S21	e.g. extruder barrels, centrifuged
1.4122	X35 Cr Mo 17	–	–	high strength parts for 300 °C, eg. small extruder screws
1.4306	X2 Cr Ni 1911	304L	304SII	stainless st., not for welding
1.4541	X6 Cr Ni Ti 1810	321	321S31	St. steel, good weldability
1.4571	X6 Cr Ni Mo Ti 1801	316Ti	320S31	higher corrosion resistance as before
1.4841	X15 Cr Ni Si 250	314/310	314S25	st. steel, good weldability
1.4542	X5 Cr Ni Cu Nb 174	630 = 17-4HP	– 431S29	melt spinnerets hardenable (formerly 1.4580)
1.4057	X22 Cr Ni 17	431		
1.4462	X2 Cr Ni Mo N 22	–	318S13	low chlorinated water (<80 ppm Cl, <180 °C)
1.4577	X5 Cr Ni Mo Ti 2525	–	–	st. steel for viscose equipm. (CV)

11. Sealing materials, gaskets
    In general, for pressure or vacuum appli-
    cation

up to ca. 80 °C   soft (synthetic) rubber
up to ca. 180 °C   silicone rubber
up to ca. 220 °C   PTFE (e.g., Teflon®)
up to ca. 300 °C   PTFE, metal-bordered, probably armored by glass
≥ 300 °C   or metal powder
                             metal on metal

– for polymer or pre-product   Al 99.5 (better: Al 99.9)
  transporting parts: for up to 200 °C
                          300 °C   AlMn 1.5
                          400 °C   AlMn1Si1.5 (if possible, with 0.2% Zr)
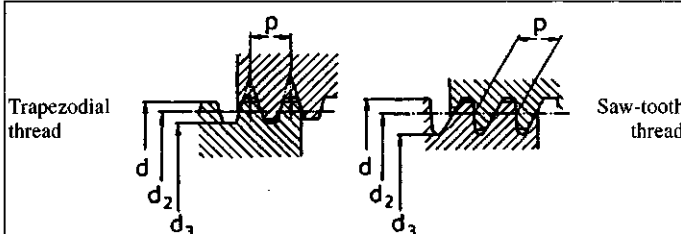   500 °C   Cu, Ni-plated (1 . . . 3 fold)
                          600 °C   1.4541

For special purposes, optimized materials must be selected, e.g., acc. to [73, 82].

7.12   High Temperature Threads

Bolts which need to be screwed at 20, as well as at 300 to 350 and possibly even at 450 °C, and need to retain sufficient load-bearing strength at these higher temperatures (for example, for sealing spin pack blocks at 400 bar internal pressure), must have trapezoidal—or saw-toothed threads dimensioned according to Table 7.15. From experience, the nut threads should always be made according to DIN/ISO,

Table 7.15   High Temperature Threads (250...350 °C), screwable

Trapezodial thread — Saw-tooth thread

Bolt threads (single thread)

Nominal diameter range mm	Pitch p	Effective diameter d	Flank diameter d_2	Core diameter d_3 Trapezodial	Core diameter d_3 Saw-tooth
20...26	2	−0.3			
28...60	3	−0.5	−0.2	−4.0	−4.75
63...100	4	−0.75	−3.0	−5.25	−6.24
105...170	6	−1.0	−4.0	−8.0	−9.49
180...240	8	−1.2	−5.5	−10.2	−12.19
250...330	10	−1.5	−7.0	−12.5	−15.00
340...400	12	−1.8	−8.7	−15.3	−18.28

Example Tr 200 × 8: d (bolt, eff.): 200 − 1.2 = 198.8 mm
  d_2 (flank): 200 − 5.5 = 194.5 mm
  d_3 Trapezoidal : 200 − 10.2 = 189.8 mm
S 200 × 8: d_3 Saw-tooth: 200 − 12.19 ∼ 187.8 mm
Nut Thread
Trapezodial threads: acc. to DIN 103 (metric, 150)
Saw-tooth threads: acc. to DIN 513

and the bolts threads should always have a smaller diameter than the nominal diameter, as given in Table 7.15. Using such bolts, the spin pack block can be hot-torqued in a hydraulic press.

The same dimensions are valid for bolts in non-threaded bores.

References

1. AEG, AG, Frankfurt/Main, Germany
2. BBC Brown Boveri AG ASEA BROWN BOVERI-Gruppe, Mannheim, Germany
3. Berges electronic GmbH, Marienheide, Germany
4. EW Hof, Hof/Saale, Germany
5. Flender AG, Bocholt, Germany
6. Gensheimer: GUSA-Getriebe, Altleiningen/Pfalz, Germany
7. Hans Heynay GmbH, Munich, Germany
8. Karl Kaiser GmbH + Co. KG, Neumünster, Germany
9. Lenze GmbH + Co. KG, Extertal, Germany
10. PIV Reimers KG, Bad Homburg v.d.H., Germany
11. PRYM, Stolberg/Rhld., Germany

12. Siemens AG, Erlangen, Germany
13. Stöber, Pforzheim, Germany
14. Voith GmbH, Heidenheim, Germany
15. Review: Stufenlose mechanische Getriebe, from "Antriebstechnik", **18** (1970) p. 300
16. Felten und Guilleaume Energietechnik AG, Cologne, Germany
17. Reiter AG, Winterthur/Switzerland
18. Schmidt, Kaiser GmbH, Neumünster: Reluktanzmotore; Lecture 1990 at [8]
19. BBC Handbook: Elektromotoren 2
20. Astro GmbH, Bremerhaven, Germany
21. Holec, Bad Muskau, Germany
22. BARMAG, Remscheid, Germany
23. Feldmühle AG, Plochingen/Neckar: Catalogue: SPK-Fadenführer
24. Rauschert GmbH + Co. KG, Pressig: Catalogue: RAPAL-Fadenführer
25. ALSiMAG Technical Ceramics, Inc., Laurens/USA
26. Kyocera Corp., Kyoto/Japan, catalog: Thread Guide
27. Télémechanique, Groupe Schneider, Ratingen, Germany
28. Electrotex AG, Obernonen, Germany
29. Molykote, Dow Corning GmbH, Munich, Germany
30. Fourné Maschinenbau GmbH, Alfter, Germany
31. Automatik Wicklerbau GmbH, Hürth-Efferen, Germany
32. *Schwab, M. E.; Heimann, P.:* Präzisionsapparate für die Chemiefaser-Industrie; CTI, 1981, p. 724
33. Enka Tecnica, Heinsberg, Germany
34. Neumag GmbH, Neumünster, Germany
35. Du Pont de Nemours & Co., Inc., Wilmington, DE/USA
36. DB-OS 1 685 664 (Glanzstoff AG)
37. Dutch Pat. 7 002 526 (Du Pont de Nemours & Co.)
38. Partex Corp., Charlotte, NC/USA
39. Heberlein AG, Wattwil/Switzerland
40. Comoli Fermo + Figli S.A.S., Paruzzaro (NO)/Italy
41. Hütte: Physikhütte, Bd.I, Mechanik, Verlag Wilhelm Ernst & Sohn, Berlin, 1971, p. 438
42. Teijin Seiki Co., Ltd., Osaka/Japan: High speed winder catalog
43. DRP 189 001 (*Jannin*)
44. Dobson + Barlow Ltd.: Platts Bull. **5** (1947) p. 195
45. *Götze K.:* Chemiefasern nach dem Viskoseverfahren, 3rd ed., Vol. 2, p. 901
46. DRP 236 584 (Vereinigte Glanzstoff-Fabriken AG, Boos)
47. US Pat. 1 770 750 and 1 800 828 (*Furness* and [45], p. 908)
48. *Prandtl, L.; Oswatisch, K.; Wieghardt, K.:* Führer durch die Strömungslehre, 8th ed., Vieweg & Sohn, Braunschweig, 1984
49. *Geiger & Scheel:* Handbuch der Physik, Bd. VII: Mechanik der flüssigen und gasförmigen Körper, J. Springer-Verlag, Berlin, 1927
50. Fourné Maschinenbau GmbH, Alfter, Germany
51. *Falkai, B., v.:* Synthesefasern, Verlag Chemie, Weinheim, 1981, p. 394
52. Schott Geräte-GmbH, Hofheim a. Ts., Germany
53. *Höllbacher, P.; Wagner, D.:* Automatische Verdünnungsviskosimetrie, Labor Praxis, no. 10, October 1981, Vogel-Verlag
54. *Klare, H.; Fritsche, E.; Gröbe, V.:* Synthetische Fasern aus Polyamiden, Akademie-Verlag, Berlin, 1963, p. 200
55. *Ludewig, H.:* Polyesterfasern, Akademie-Verlag, Berlin, 1975, p. 193
56. Karl Fischer Industrieanlagen GmbH, Berlin, Taschenkalender 1990
57. USTER-Gleichmäßigkeitsprüfung, Handbuch 9.81/400 [60]
58. USTER-Gleichmäßigkeitsprüfung, für Filamentgarne, Handbuch 3.86/208 [60]
59. Mathematically, $CV = \dfrac{1}{\bar{X}} \sqrt{\dfrac{1}{T} \int_0^T (x_i - \bar{x})^2 \, dt}$
60. Zellweger-Uster AG, Uster/Switzerland
61. *Schollmeyer, E.; Knittel, D.; Hemmer, E. A.:* Betriebsmeßtechnik in der Textilerzeugung und -veredlung; Springer Verlag, Berlin, 1988
62. Dr. Henschen GmbH + Co., Sindelfingen, Germany
63. Dynisco Inc., Norwood, Mass./USA or Dynisco Geräte GmbH, Heilbronn-Neckargartach, Germany

64. *Whelan, T.; Dunning, D.:* The Dynisco Extrusion Processors Handbook, 1st ed. 1988, Dynisco Inc. [63]

65. *Homann, F.:* Forschung auf dem Gebiet des Ing.-Wesens 7 (1936)

66. Wieghardt; University Hamburg

67. Gebr. Kufferath, Düren/Rhld., Germany

68. *Syben, N.:* Möglichkeiten zur Dämpfung von Geschwindigkeitsschwankungen der Blasluft bei Synthesefaser-spinnverfahren, Fachhochschule Aachen, Abt. Maschinenbau, Report no. 3050, 1974

69. *Dryden, H. L.; Schönbauer,* in *Schlichting, H.:* Grenzschichttheorie; Verlag C. Braun, Karlsruhe, 1958

70. *Prandtl L.:* Strömungslehre, 4th ed., Viehweg & Sohn, Braunschweig, 1944, p. 101

71. Deutsches Textilforschungszentrum Nord-West e.V.: Charakterisierung von textilen Flächengebilden für den kontinuierlichen Produktauftrag durch Untersuchung des Stoffaustausches in Abhängigkeit von der Strömungsmechanik beim Foulardieren; DTNE-Nr. 113, Krefeld, October 1986

72. Creushot-Loire Industrie, Paris-la-Défense/France

73. *Wellinger, K.; Gimmel, P.; Bodenstein, M:* Werkstoff-Tabellen der Metalle, Alfred Kröner-Verlag, Stuttgart, 7th ed.

74. *Vogel, J.:* Grundlagen der elektrischen Antriebstechnik mit Berechnungsbeispielen, Hüthig-Verlag Heidelberg, 4th ed., 1989

75. *Bauer, W.:* Was man bei der Festlegung der Typengröße von thyristorgespeisten Thyristormotoren beachten muß, issued by Baumüller, Nürnberg, Germany

76. *Hoffmann, M.; Kröhner, H.; Kuhn, R.:* Polymeranalytik II Georg Thieme-Verlag, Stuttgart, 1977

77. *Flory, P. J.:* Viscosities of linear Polyesters—exact relationship between viscosity and chain length, J. Amer. Chem. Soc. **62**, (1940) p. 1957

78. *Buechle, F.:* Viscosity of Polymers in concentrated solution, J. Chem. Phys. **25** (1956) p. 599 and J. Polymer Sci. **41** (1959) p. 551

79. *Fox, T. G.; Flory, P. J.:* Viscosity-Molecular Weight and Viscosity-Temperature Relationships for Polystyrene and Polyisobutylene, J. Amer. Chem. Soc. **70** (1948) p. 2384

80. *Kochomskaja, T. N.; Paksver, A. B.:* Kolloid Zh. (Russian) **18** (1956) 2, p. 188

81. *Fourné, F.:* Einige Ursachen von Titer-, Dehnungs- und Färbeschwankungen: Chemiefasern/Textilindustrie, June 1984, p. 419

82. Stahlschlüssel: Verlag Stahlschlüssel, Marbach, latest edition (also for comparison with non-German materials)

83. Edmund Erdmann Elektrotechnik, Mülheim/Ruhr, Germany

84. Göttfert Werkstoff-Prüfmaschinen GmbH, Buchen, Germany

85. *Bobeth, W.:* Textile Faserstoffe; Springer-Verlag Berlin, 1993

86. *Fourné, F.* (nach Pieper, R.): Synthetische Fasern; Konradin-Verlag Robert Kohlhammer, Stuttgart 1953

87. Preßmetall Krebsöge GmbH, Radevormwald, Germany

88. DIN VDE 0160, German electrotechnical commission, DIN and VDE (DKE), draft December 1990

89. DIN 1310, Din 53800, 53822...25

90. *Bobeth, W.:* Textile Faserstoffe; Springer-Verlag, Berlin 1993, p. 231 ff.

91. *Lünenschloß, J.:* Lecture "Textiles Prüfwesen" May, 1979, at the RWTH Aachen, Institut für Textiltechnik

92. Brabender Meßtechnik KG., Duisburg, Germany, Catalog: "Aquatrac Moisture Meter", Oct., 1996

93. BASF or DSM: Catalog: "Caprolactam"